Waqas Ali

Speed control of electrical drives with resonant loads
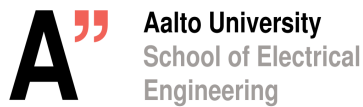
School of Electrical Engineering

Master's Thesis submitted in partial fulfillment of the requirement for the degree of Master of Science in Technology.
Espoo 02.06.2011

Thesis supervisor:

Dr. Marko Hinkkanen

Thesis instructor:

Seppo Saarakkala, M.Sc. (Eng.)

A" Aalto University
School of Electrical
Engineering

Author:	Waqas Ali	
Title:	Speed control of electrical drives with resonant loads	
Date: 02.06.2011	Language: English	Pages: 10 + 56
Department of Electrical Engineering		
Professorship: Electrical Drives		Code: S-81
Supervisor: Dr. Marko Hinkkanen		
Instructor: Seppo Saarakkala, M.Sc. (Eng.)		

This thesis deals with the speed control methods of electrical drives with resonant loads such as rolling mill drives with long shafts, robotic arms with flexible couplings and elevators with flexible ropes. The electrical drive with a resonant load is modeled as a two-mass resonant system. Three speed controlling techniques have been designed: a state-space controller, a two-degree-of-freedom (2DOF) controller tuned according to the rigid system model; and a 2DOF controller tuned according to the flexible system model. The state-space controller is designed based on the pole placement technique and with the assumption that all state variables are available. Both 2DOF methods include PI feedback controllers, where two different feedforward controllers are considered. The design principles and analytical tuning methods of the controllers are presented. Three simulation studies are carried out to test and analyze the reference-tracking capabilities and sensitivity to disturbances of the designed speed controllers. Finally, the benefits and limitations of the speed controllers as well as some recommendations for future research areas are presented.

Keywords: Speed control, two-mass resonant system, state-space control, two-degree-of-freedom control, flexible systems, electrical drives.

i

Acknowledgements

The work in this Master's thesis was carried out at Aalto University School of Electrical Engineering under the supervision of Dr. Marko Hinkkanen.

First of all, thanks should be forwarded to God, most gracious, most merciful, who guides me in every step I take. I would like to express my deepest gratitude to Professor Jorma Luomi for accepting and giving me this wonderful research project, my supervisor Dr. Marko Hinkkanen whose supervision both helped me to channel and specify the discussed ideas and at the same time provided much appreciated freedom and support to explore new ways and concepts. His endless drive for new and better results is highly appreciated. I would like to take this opportunity to acknowledge my instructor Mr. Seppo Saarakkala, M.Sc. (Eng.) for all his guidance and encouragement. Several ideas in this dissertation have been benefited from his insightful discussions. I am very grateful for his endless support, positive and motivating attitude and for his kind assistance throughout. I also would like to thank Mr. William Martin for linguistic editing and proofreading my thesis.

My gratitude to all my friends for their joyous company specially to my friend Mr. Muhammad Yasir who has been supportive and motivating for me.

Many thanks to my brother Mr. Shahzad Ali who has been a pillar of support and comfort during this hard time. Finally, I would like to thank my parents and whole family, who have always been by my side and provided me with unwavering support throughout my life.

Espoo, 02.06.2011.

Waqas Ali

Abbreviations and symbols

A	System matrix
B	Input matrix
C	Output matrix
C_S	Shaft damping coefficient
D	Feedthrough matrix
J_L	Load inertia
J_M	Motor inertia
K_J	Inertia ratio
K_R	Resonance ratio
K_S	Shaft stiffness
s	Laplace variable
T_L	Load torque
T_M	Motor torque
T_S	Shaft torque
u	Input vector
x	State vector
α	Angular acceleration
α_s	Bandwidth of 2DOF rigid system model
ϵ	Difference between motor and load angular positions
ζ	Damping ratio
θ_L	Load angular position
θ_M	Motor angular position
ω_A	Anti resonance frequency
ω_L	Load speed
ω_M	Motor speed
ω_R	Resonance frequency

Acronyms

PI	Proportional-integral
PID	Proportional-integral-derivative
1DOF	one-degree-of-freedom
2DOF	Two-degree-of-freedom
MRAC	Model reference adaptive control

Contents

List of Tables

List of Figures

Chapter 1

Introduction

1.1 Background

In the modern industrial world, motion control (speed, position) is very important to enhance productivity, quality and to reduce energy consumption as well as equipment maintenance. Its application fields are widely present in industry such as pick and place tasks and robotic arms. Electrical drives have a major share in most industrial motion control applications and industrial robots as these perform the conversion of electrical energy into mechanical energy or vice versa in various processes. These drives may operate at constant speed or at variable speeds, depending upon the utilizing process, and are considered crucial components in almost all industrial applications.

A significant improvement has been observed in control technology and strategies of electrical drives during the last two decades. The technological progress in the industrial world has amplified demand for flexibility and precision as well as requirement of energy loss minimization due to the global energy crisis. The ease of controlling the electrical drives is an important factor in order to meet these requirements. This trend owes its progress to the various philosophies and techniques, developed by several researchers around the world, such as the PID/PI control scheme, the adaptive control scheme, and the resonant ratio control scheme.

In many industrial and robotics applications, the mechanical parts of drive systems may have very low resonant frequency, such as rolling mills which normally comprise of a long shaft and large load-side mass, elevators with flexible transmission rope or industrial robotic arms having flexible coupling. A light weight and high load-to-weight ratio construction is required in in-

dustrial robots for fast motion and high efficiency in operation. For these reasons, the dynamics of such systems should be modeled as two-mass or multi-mass systems. The speed control of such systems has significant interest in the scientific community due to their importance in the industrial world. The main tasks of speed controllers are: tracking of the speed reference, rejection the effect of load torque and suppression of shaft torsional vibration.

1.2 Scope

Typical industrial motor drive systems may contain several mechanical couplings between a motor and a load. The couplings are not stiff. These drive systems are increasingly required in industrial automation. However the structural resonance of the drive system is easily excited by rapid change in speed. When flexibility is considered, these drive systems can be modeled as two-mass resonant systems.

A number of strategies have been proposed to design a speed controller for the two-mass resonant systems. A basic control structure is PI control. Usually, all state variables are not available as well as it is not easy to achieve analytical design. Also it is hard to develop a unified method to deal with various demands. Therefore, it is highly desirable to have an easy-to-tune controller which has the ability to control a drive system according to the requirements of the process.

1.3 Objective

The prime objective of this Master's thesis is to design, implement and evaluate the performance of a two-degree-of-freedom (2DOF) PI speed controller for a two-mass resonant system with two different tuning methodologies so as to meet the requirements for typical industrial motor drive systems. The parameters of the controller will be tuned by following two different methodologies:

- Parameter tuning according to a rigid system model.

- Parameter tuning according to a flexible system model.

This designing evaluation should be done theoretically and through simulation. Since the state-space controller can be considered as the best controller

if all state variables are available, we will use it as a benchmark. The performance of the 2DOF PI speed controller will be compared with the performance of this controller. Hence, it is also required to design a state-space controller while assuming that all state variables can be measured and are available for controller design.

The designed 2DOF PI speed controller must possess the following characteristics:

- Fast tracking of the load speed with respect to the reference speed without overshoot.

- Reject the effect of the load torque.

1.4 Disposition

This Master's thesis consists of five chapters. The first chapter provides a brief introduction of the thesis. Chapter 2 introduces the model of a two-mass resonant system. The prime objective of this thesis begins in Chapter 3 where various related control strategies and techniques proposed in the scientific community are briefly reviewed. Then, a state-space controller is designed and finally two parameter tuning techniques for the 2DOF PI controller are explained for a two-mass resonant system. Chapter 4 contains performance comparison of the designed controllers based on the simulation results. Finally, the thesis is concluded in Chapter 5.

Chapter 2

Modeling of the two-mass resonant system

In this chapter, the structure and the model of a two-mass resonant system is explained. The block diagram of the system is described followed by a brief review of the open loop frequency response of the system.

2.1 Two-mass resonant system

A simple structure of a two-mass resonant system is shown in Fig. 2.1. The system comprises of the motor and the load, connected through a flexible shaft or transmission element. This flexible shaft or transmission element has non-ideal transmission behavior such as finite torsional stiffness. This finite stiffness can cause unwanted torsional oscillations as well as can stress both the mechanical and electrical components of the system. The mechanical parts of such systems may have a low resonant frequency so the structural resonance is easily excited by rapid change is speed.

Consider a two-mass resonant system where J_M is motor inertia, J_L is load inertia, ω_M is motor speed, ω_L is load speed, T_M is motor torque, T_L is load torque, T_S is shaft torque, K_S is shaft stiffness, C_S is the shaft damping coefficient, θ_M is motor angular position and θ_L is load angular position. (Leonhard, 1996), (Shahgholian et al., 2009b)

The equation representing the motor dynamics is

$$J_M \frac{d}{dt} \omega_M = T_M - T_S. \tag{2.1}$$

4
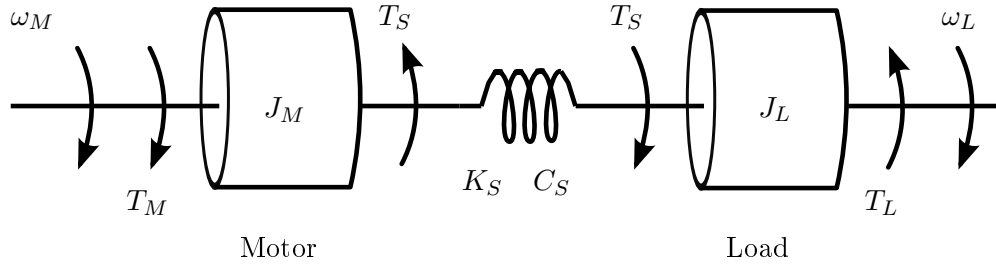
Figure 2.1: Two-mass resonant system.

The equation representing the load dynamics is

$$J_L \frac{d}{dt}\omega_L = T_S - T_L. \tag{2.2}$$

During the motion, the speed ω_M and angular position θ_M of the motor shaft differ from respective variables ω_L and θ_L on the load side. Hence, the torsional torque is given by

$$T_S = K_S \epsilon + C_S(\omega_M - \omega_L), \tag{2.3}$$

where ϵ is the difference between the motor and load angular positions

$$\epsilon = \theta_M - \theta_L. \tag{2.4}$$

The speed of the motor ω_M and the speed of the load ω_L are respectively

$$\frac{d}{dt}\theta_M = \omega_M \tag{2.5}$$

$$\frac{d}{dt}\theta_L = \omega_L. \tag{2.6}$$

In this model, the viscous damping coefficients of the motor and the load are being neglected as the damping of the system is low and analysis accuracy is not affected by neglecting the friction. (Zhang and Furusho, 2000)

2.2   State-space representation

A state-space representation of the system is given by the following equations and is shown in Fig. 2.2.
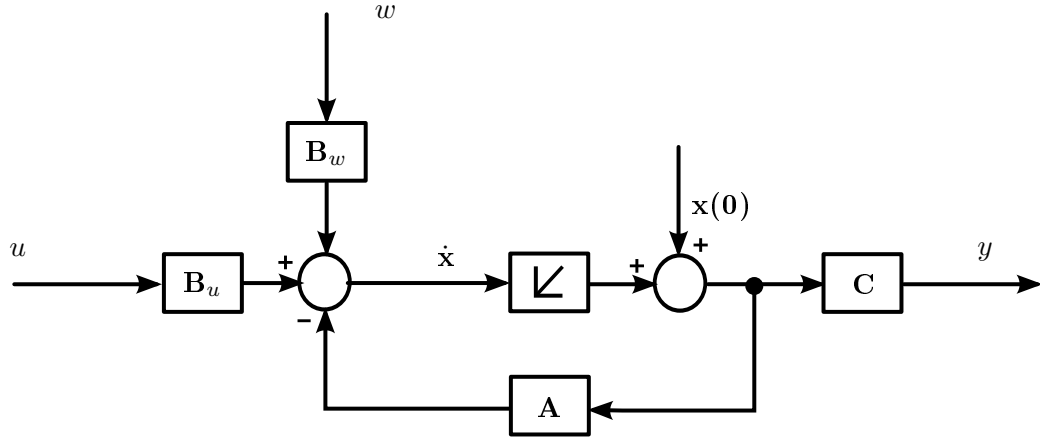
Figure 2.2: State-space representation as block diagram.

$$\dot{\mathbf{x}} = \mathbf{A}\mathbf{x} + \mathbf{B}_u u + \mathbf{B}_w w \tag{2.7}$$

$$y = \mathbf{C}\mathbf{x}, \tag{2.8}$$

where $\mathbf{x}$ is the state vector, $\mathbf{u}$ is the input vector, $\mathbf{A}$ is the system matrix, $\mathbf{B}_u$ and $\mathbf{B}_w$ are the input matrices and $\mathbf{C}$ is the output matrix. If a system has n number of states, m number of inputs and r number of outputs then the orders of these matrices are given as: $\mathbf{A}$ is $n \times n$ matrix, $\mathbf{B}$ is $n \times m$ matrix and $\mathbf{C}$ is $r \times n$ matrix. (Buchi, 2010)

The state vector $\mathbf{x}$ includes three state variables: the motor speed ω_M, the load speed ω_L and the difference of the angular positions between the motor and the load ϵ. The control u equals the control input T_M and w equals the disturbance input T_L. The output is y. The state-space model of a two-mass resonant system is

$$\frac{d}{dt} \begin{bmatrix} \omega_M \\ \epsilon \\ \omega_L \end{bmatrix} = \underbrace{\begin{bmatrix} -\frac{C_S}{J_M} & -\frac{K_S}{J_M} & \frac{C_S}{J_M} \\ 1 & 0 & -1 \\ \frac{C_S}{J_L} & \frac{K_S}{J_L} & -\frac{C_S}{J_L} \end{bmatrix}}_{\mathbf{A}} \underbrace{\begin{bmatrix} \omega_M \\ \epsilon \\ \omega_L \end{bmatrix}}_{\mathbf{x}} + \underbrace{\begin{bmatrix} \frac{1}{J_M} \\ 0 \\ 0 \end{bmatrix}}_{\mathbf{B}_u} \underbrace{\begin{bmatrix} T_M \end{bmatrix}}_{u} + \underbrace{\begin{bmatrix} 0 \\ 0 \\ -\frac{1}{J_L} \end{bmatrix}}_{\mathbf{B}_w} \underbrace{\begin{bmatrix} T_L \end{bmatrix}}_{w}$$

$$\tag{2.9}$$

$$\mathrm{y} = \underbrace{\begin{bmatrix} 0 & 0 & 1 \end{bmatrix}}_{\mathbf{C}} \begin{bmatrix} \omega_M \\ \epsilon \\ \omega_L \end{bmatrix}. \tag{2.10}$$

2.3   Transfer function representation

From the state equations, the transfer function of the system can be calculated as

$$G(s) = \frac{Y(s)}{U(s)} = \mathbf{C}(s\mathbf{I} - \mathbf{A})^{-1}\mathbf{B}_u. \tag{2.11}$$

A two-mass resonant system can easily be modeled by functional blocks. Considering a two inputs and single output system, the block diagram of the two-mass resonant system can be represented as in Fig. 2.3.

Considering (2.11), the open loop transfer function from the motor torque to the motor speed can be calculated, if we select the matrix $\mathbf{C}$ as

$$\mathbf{C} = \begin{bmatrix} 1 & 0 & 0 \end{bmatrix}, \tag{2.12}$$

and given in the form

$$\frac{\omega_M(s)}{T_M(s)} = \underbrace{\frac{1}{s(J_M + J_L)}}_{\text{Rigid part}} \underbrace{\frac{s^2 J_L + sC_S + K_S}{s^2 \frac{J_M J_L}{J_M + J_L} + sC_S + K_S}}_{\text{Flexible part}}. \tag{2.13}$$

The transfer function can be assumed to consist of the two parts: the rigid part and the flexible part. Similarly the open-loop transfer function from the motor torque to the load speed can be calculated, if we select the matrix $\mathbf{C}$ as

$$\mathbf{C} = \begin{bmatrix} 0 & 0 & 1 \end{bmatrix}, \tag{2.14}$$

and given as

$$\frac{\omega_L(s)}{T_M(s)} = \underbrace{\frac{1}{s(J_M + J_L)}}_{\text{Rigid part}} \underbrace{\frac{sC_S + K_S}{s^2 \frac{J_M J_L}{J_M + J_L} + sC_S + K_S}}_{\text{Flexible part}}. \tag{2.15}$$

The characteristic equation $\Delta(s)$ can be given as

$$\Delta(s) = s(s^2 + 2\zeta_n \omega_R s + \omega_R{}^2). \tag{2.16}$$
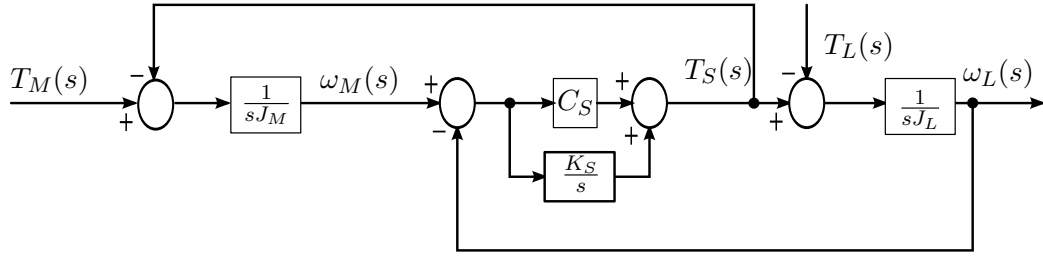
Figure 2.3: Block diagram of the two-mass resonant system.

The resonance frequency ω_R and damping ratio ζ_n are given by

$$\omega_R = \sqrt{\frac{K_S}{J_L}(1+R)} \quad , \quad \zeta_n = \frac{C_S}{2}\sqrt{\frac{1}{K_S J_L}(1+R)}, \qquad (2.17)$$

where $R = J_L/J_M$ is inertia ratio. The anti-resonance frequency is given as

$$\omega_A = \sqrt{\frac{K_S}{J_L}}. \qquad (2.18)$$

The anti-resonance frequency is lower than the resonance frequency. Phase characteristics of the system change drastically at these frequencies. Excitations change with motor-inverter speed, despite the fact that the natural frequencies are constant. The resonance characteristics can be explained by its resonance ratio K_R which is given

$$K_R = \frac{\omega_R}{\omega_A} = \sqrt{1 + \frac{J_L}{J_M}}. \qquad (2.19)$$

If we have $J_M \gg J_L$, then the torsional torque oscillations are filtered by the large motor inertia J_M and the influence of the oscillations on the speed control becomes smaller. In closed-loop motion control, the control bandwidth of the system is limited by the anti-resonance frequency ω_A. If the motor inertia J_M increases then the resonance frequency ω_R decreases, without having any affect on the anti-resonance frequency ω_A. On the other hand, both frequencies ω_R and ω_A increase with the increase in the mechanical stiffness of the shaft K_S as well as mechanical bandwidth increases in the closed-loop system. (Shahgholian et al., 2009a),(Shahgholian et al., 2009b)

2.4 System parameters and frequency response

In this thesis, we are using the parameters for the two-mass resonant system given in Table 2.1.

Table 2.1: Two-mass resonant system parameters.

Parameter	Symbol	Value	Unit
Motor inertia	J_M	0.0044	kgm^2
Load inertia	J_L	0.0360	kgm^2
Shaft stiffness	K_S	30	Nm/rad
Shaft damping coefficient	C_S	0.05	Nm/rad

An open-loop frequency response from the motor torque to the motor speed can be obtained by (2.13) and shown in Fig. 2.4, using the system parameters given in Table 2.1. The open-loop frequency response from the motor torque to the load speed by (2.15) is shown in Fig. 2.5.

It can be seen from the frequency response that the system is highly under damped. From the characteristic equation (2.16), the natural frequencies and the damping for the poles of system can be calculated. The open-loop system has three poles. One pole is in origin where as the resonant pole pair has the frequency $\omega_R = 87.5$ rad/sec and the damping $\zeta = 0.0729$ which is a very small value, indicating that the system is poorly damped.
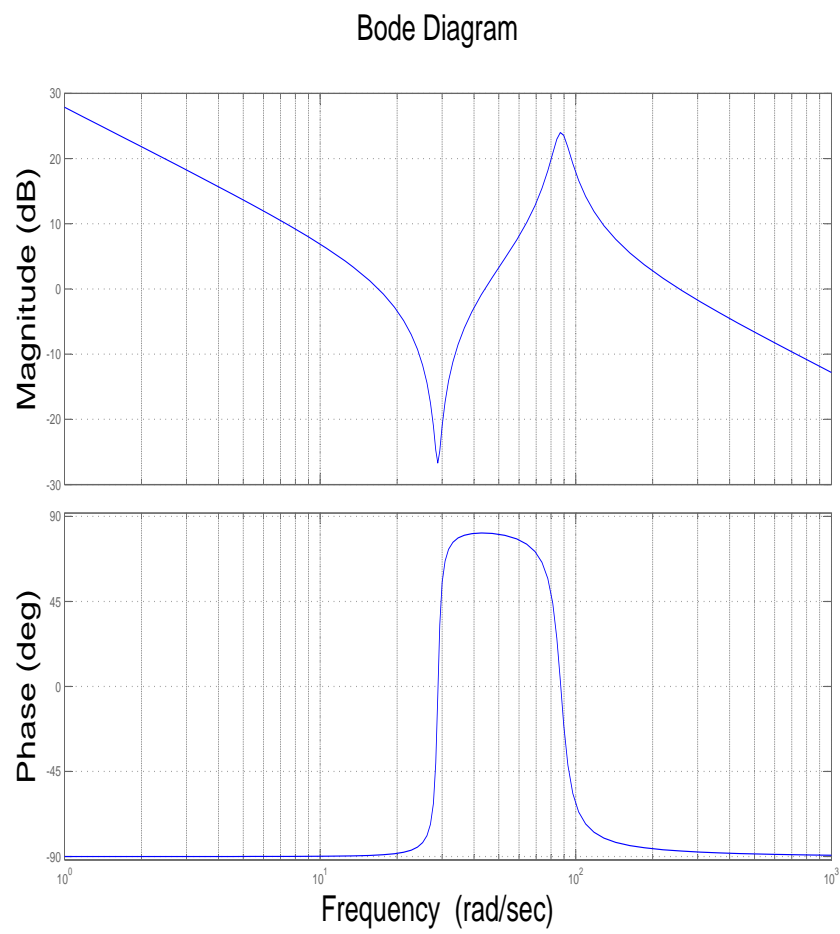
Figure 2.4: Open-loop frequency response from the motor torque to the motor speed.
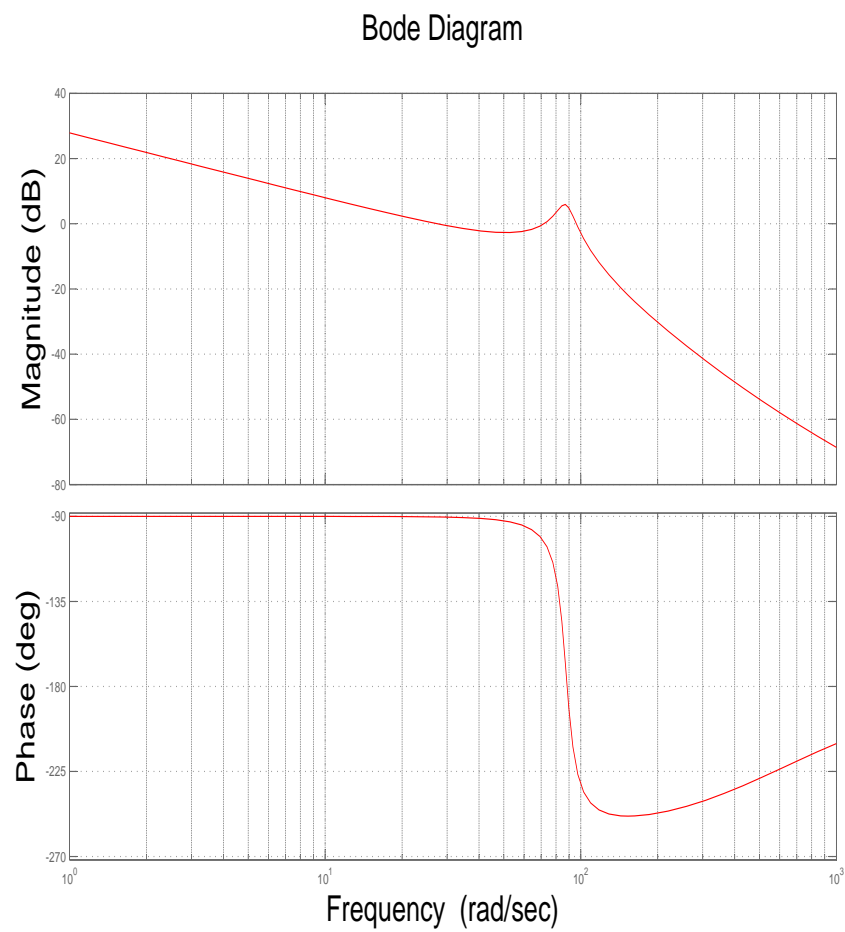
Figure 2.5: Open-loop frequency response from the motor torque to the load speed.

Chapter 3

Speed control of two-mass resonant system

In this chapter, first a brief literature review of various speed control strategies for a two-mass resonant system is presented. After that, a pole placement state-space controller design is described. Then, one-degree-of-freedom (1DOF) and 2DOF control designs are discussed. For the 2DOF controller design, a feedforward-type structure is used. Finally, two parameter tuning methods of the PI-type 2DOF controller are presented.

3.1 Control strategies for the two-mass resonant system

A number of control topologies have been proposed to control the two-mass resonant systems. In many industrial and robotics applications, a light weight and high load-to-weight ratio construction is required for fast motion and high efficiency in operation while considering the fact that the mechanical parts of the drive systems may have a low resonant frequency.

For these reasons, the dynamics of such systems should be modeled as two-mass or multi-mass systems. The speed control of such systems has significant interest in the scientific community due to importance and prevalence of these systems in the industrial world. The prime objectives of the speed controllers are: fast tracking of the speed reference, rejection the effect of the load disturbance torque and suppression of the shaft torsional vibration.

Several methods and techniques have been described by researchers to con-

trol the two-mass resonant system such as using PI/PID controllers, PI-speed controller with additional feedback, a state-feedback speed control system with and without state observers, an adaptive control scheme, adaptive sliding mode neuro-fuzzy control without mechanical sensors and 2DOF controllers. A brief description of these control structures is presented here.

Dhaouadi et al. (1993) have presented a scheme of the 2DOF speed controller for rolling mills drives. This 2DOF controller uses an observer based state-feedback compensator for major control loop. It is considered that all state variables are available. They used a set-point filter type 2DOF structure for speed controller. Control law design is implemented by the combination of integral control compensation and load disturbance feedforward compensation. For state-feedback gain design, the pole-placement technique is used. A roll-off filter is used to reduce the system gain beyond the cut-off frequency of the system. This speed controller was designed with low overshoot (i.e. 10%).

Kim et al. (1996) have described a 2DOF speed control method of the two-mass resonant system, based on the induction machine. For the speed control of the induction motor, the vector control theory is used. The state observer is constructed from the motor speed which is measured by the speed sensor and the torque producing current. This state observer estimates the load speed, the shaft torsional torque and the load disturbance torque. A feedback controller is designed using these state variables. In order to improve the speed response a feedforward controller is also designed by using the one-mass system, neglecting the shaft torsional vibration. The complete control structure is a 2DOF speed controller. In this controller, the feedback controller is responsible for the internal stability of the system and the feedforward controller is designed for fast speed response to the command. This 2DOF controller is compared with the state-feedback controller and it is shown that it is more robust on load disturbance torque and shaft torsional vibrational as well as contains a fast speed response property.

Hara et al. (1997) provided a comparison for the state feedback-based speed control systems with state observers and without state observers in the motor drives. They have presented a design for a robust state feedback-based speed control system considering the stability condition and frequency response wave shaping. This state-feedback controller is designed by using only measureable state variables without a state observer and denoted as a partial state-feedback controller. The optimal feedback gains are determined by evaluating the appropriate area on the parameter plane, called the gain area, using Hurwitz stability criterion. Then they have presented a com-

Table 3.1: Relationship between the damping behavior and the inertia ratio. (Zhang and Furusho, 2000)

Pole assignment pattern	Inertia ratio			
	$R < 1$	$1 \leq R < 2$	$2 \leq R \leq 4$	$R > 4$
Identical radius	Under damped	Under damped	Well damped	Impossible
Identical damping coefficient	Under damped	Under damped	Well damped	Well damped and over damped
Identical real part	Under damped	Well damped	Well damped	Impossible

parison between the state-feedback controller and the partial state-feedback controller by μ analysis. The partial state-feedback controller is not as excellent as the state-feedback controller in terms of robust stability when plant parameters are varying but it is easier to apply the partial state-feedback controller due to its simple control system structure without observers.

Zhang and Furusho (2000) have described the redesigning of a conventional PI speed controller for the two-mass resonant system. The damping characteristics of the system are derived and analyzed. They have shown the dependence of the inertia ratio of the load to motor on the dynamic characteristics of the system. Three kinds of pole placement techniques have been used:

- Pole assignment of identical radius.

- Pole assignment of identical damping coefficient

- Pole assignment of identical real part

The merits of each pole-assignment design are concluded. Finally, a method is proposed to improve the damping of the system for a small inertia ratio by a derivative feedback of the motor speed. For these three types of pole assignments, the relationship between the damping behavior and the inertia ratio is summarized and shown in Table 3.1 where $R = J_L/J_M$ is the inertia ratio.

Lee et al. (2006) have described a recursive robust control design method for the flexible joints of the industrial robots. These flexible joints can be considered as cascade systems composed of two subsystems: the link-side dynamics and the motor-side dynamics driven by the driving torque input. The controller is designed on the basis of a recursive method for the cascade system to achieve the robustness at each step. The robustness of the designed controller is compared with the conventional state feedback controller. In the design method, they have first designed a fictitious control for the link-side

dynamics and then they designed the real control for the overall system so that the motor-side dynamics effectively tracks the fictitious control. The real control part is designed as a PID-controller for the complete system.

A comparative study about vibration suppression in a two-mass resonant system from the PI-speed controller and additional feedbacks using the classical pole-placement method is described by Szabat and Kowalska (2007). In order to get access to damping, some information is required from the load side. For a two-mass resonant system, additional feedbacks are required to achieve the desired damping coefficient and resonant frequency simultaneously. Rather than using a large number of possible feedbacks, it is shown that the systems with one additional feedback can be divided into three different groups, according to their dynamic characteristics. Finally, a system with two additional feedbacks is investigated and then a comparison of the considered structures is carried out. The best dynamical characteristics are obtained by the control structure with one additional feedback, from the following possible feedbacks:

- Feedback from derivative of the torsional torque, provided to the torque node.

- Feedback from the difference between the motor and the load speeds provided to the torque node.

- Feedback from the load speed, provided to the torque node.

Shahgholian et al. (2009a) have presented a PID controller design for the two-mass resonant system by consideration of the frequency response and the step response characteristics. They have used the pole-placement technique which is based on the coefficient diagram method to assign the closed-loop poles of the system. Then, by using the relation among the coefficient of the closed-loop characteristic polynomial, the gains of the PID controller are calculated. By comparison, analysis and simulation of the PID controller and the PID controller with active damping, it is shown that a better speed response to suppress the mechanical vibrations is achieved by using the proposed PID controller tuning.

A state-space analysis and control design for the two-mass resonant system is presented by Shahgholian et al. (2009b). This methodology depends on the resonance ratio control by using optimal criterion of the system. This controller consists of the integral controller and the proportional controller with an additional feedback signal from the shaft torque. The controller

Table 3.2: Comparison of proposed speed control approaches by Thomsen et al. (2010).

Comparison criteria	PI_{SC}	$PI-SS_{SC}$	GPC_{SC}
Dynamics			
Small-signal performance	Low	Excellent	Good
Large-signal performance	Low	Good	Good
Disturbance rejection	Low	Excellent	Good
Stress of drive shaft	High	Low	Low
Stability Properties			
Relative stability	High	Excellent	Medium
Robustness concern, uncertain parameters	High	High	Medium
Calculation time	Low	Low	High
Possibilities of controller design	Low	High	Medium
Complexity of implementation and tuning	Low	High	High

bandwidth in the closed-loop motion control system is limited by the anti-resonant frequency of the system. The controller gains are obtained by the coefficient diagram method which is an indirect pole-placement method to design an appropriate characteristic polynomial.

Thomsen et al. (2010) presented a comparative study of different control strategies of the two-mass resonant systems. They describe and compare three different control methods: the conventional PI control (PI_{SC}), the PI-based state-space control ($PI-SS_{SC}$) and the generalized predictive control (GPC_{SC}). For suitable comparison, the three controller types are designed with equal bandwidth and verified with the same test setup. The results are shown in Table 3.2. The conventional PI-control system provides a low control performance and high stress on the mechanical system but it is easy to design and implement. More effective results are achieved by the GPC_{SC}. The limitation of GPC_{SC} is the required online time calculation. The best results are concluded for the PI-based state-space control design due to its free pole placement but for this scheme an observer for the estimation of the non-measured states is required.

Orlowska-Kowalska et al. (2010) has presented a sliding-mode neuro-fuzzy speed controller, whose connective weights are tuned online according to the error between the estimated motor speed and the reference model speed for the two-mass induction motor drives without mechanical sensors. The effectiveness of this adaptive sliding mode neuro-fuzzy speed controller is described. A gradient descent algorithm is used according to the error between

the estimated speed and the reference model output to tune the connective weights. The speed of the induction machine is estimated using the model reference adaptive control (MRAC) scheme and the rotor speed is calculated on the basis of the error between the measured and the estimated stator currents of the motor. It is shown that the proposed controller has better performance than the conventional PI controller.

3.2   State-space controller design

In this section, a state-feedback speed controller for a two-mass resonant system is designed.

3.2.1   Control law design for full state feedback

When designing a state-space controller, the basic task is to find the control law as the feedback of a linear combination of the state variables. The purpose of the control law is to assign a set of pole locations for the closed-loop system that will correspond to a satisfactory dynamic response in terms of the rise time and other measures of the transient response. (Franklin et al., 2002)

Generally, the control law is

$$u = -\mathbf{K}\mathbf{x} = \begin{bmatrix} k_1 & k_2 & ... & k_n \end{bmatrix} \begin{bmatrix} x_1 \\ x_2 \\ . \\ . \\ x_n \end{bmatrix}. \qquad (3.1)$$

The system design with control law is shown in Fig. 3.1.

Pole-placement method

The pole-placement method is used to place the poles of a closed-loop system on the desired location by the state feedback, through the appropriate state feedback gain matrix if the given system is perfectly controllable.

This method can be applied in both cases where either the state-space model of the system is given or the related system is given by the transfer functions. The constraint for the state-feedback technique is: all state variables have to
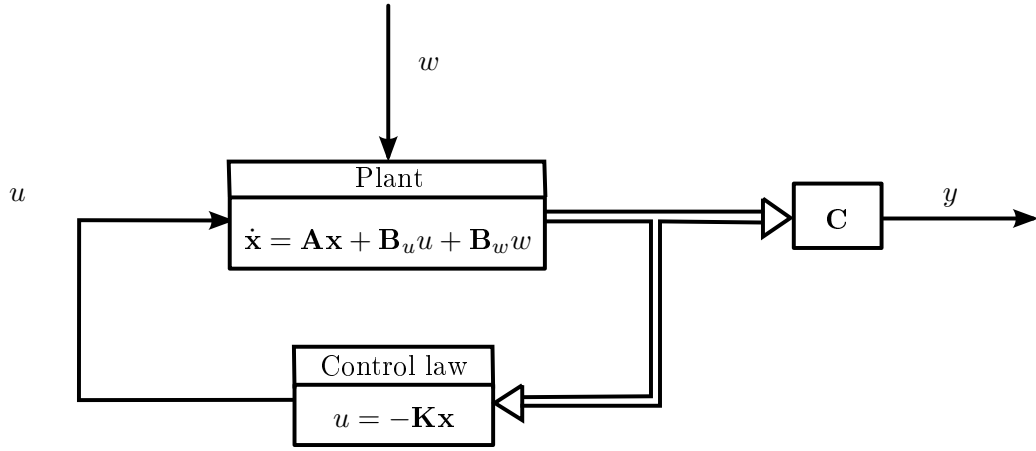
Figure 3.1: System design with control law.

be available. It is required to measure all state variables or to include the state observers into the system.

If we have a state-space model of a system as in (2.7), (2.8) and $w = 0$ then it is required to find the gain matrix (3.1) for the state-space controller. It means that the control signal is determined by the system states at each moment.

Designing of the controller requires deciding the appropriate state feedback gain matrix $\mathbf{K}$. The dimension of the gain matrix $\mathbf{K}$ is $1 \times n$ where n is the number of the system states. Now if u is substituted from (3.1) into (2.7)

$$\dot{\mathbf{x}} = (\mathbf{A} - \mathbf{B}_u\mathbf{K})\mathbf{x}. \tag{3.2}$$

The response in the time domain is

$$\mathbf{x}(t) = e^{(\mathbf{A} - \mathbf{B}_u\mathbf{K})t}\mathbf{x}(0), \tag{3.3}$$

where $\mathbf{x}(0)$ is the initial state of the system. The stability and transient response characteristics of the system are determined by the eigenvalues of the matrix $(\mathbf{A} - \mathbf{B}_u\mathbf{K})$. These eigenvalues are called regulator poles. If these regulator poles are located in the left half plane, the closed-loop system will be stable. The purpose of the pole-placement method is to obtain the gain matrix $\mathbf{K}$ by assigning the closed-loop poles of the system to appropriate locations on the left side of the s-plane in order to get the desired response of the system. (Dorf and Bishop, 2001), (Wang et al., 2009)

Selection of pole locations

An important aspect of the pole-placement design method is to decide, where to locate the closed-loop poles. The control effort required for controlling a system is related to that how far the open-loop poles are moved by feedback. Furthermore, poles are attracted by open-loop zeros, therefore it is normally hard to move a pole far away from a nearby zero.

The pole-placement design technique that aims to fix the undesirable aspects of the open-loop system response will typically allow the smaller control actuators as compared to that arbitrarily picks all the poles in some location without regard to the original open-loop poles.

There are many techniques to select the appropriate pole locations such as:

- Dominant second-order method.

- Prototype design method.

- Symmetric root locus method.

- Linear quadratic regulator (LQR) method.

The first two approaches deal with the pole selection, without explicit regard for their effect on the control effort whereas the third technique specifically addresses the issue of achieving a good balanced system response and control efforts (Franklin et al., 2002). Keeping in mind the open-loop pole locations, the first method will be used for designing a state-space controller.

Dominant pole pair design

For a higher order system, closed-loop poles can be considered as a desired pair of dominant second-order poles; the rest of the poles can be selected to have real parts corresponding to sufficiently damped modes. In this way, the system will mimic a second-order response with reasonable control efforts. By proper design it is possible to force the closed-loop poles of the higher order system to the two regions as shown in Fig. 3.2.

A complex conjugate pole pair is placed in Region 1 and all other poles are in Region 2. The pair of complex conjugate pole in Region 1 has a dominant effect on the transient response of the system and refers as the dominant pole pair of the system. The parameters ζ and ω_n of the dominant pole
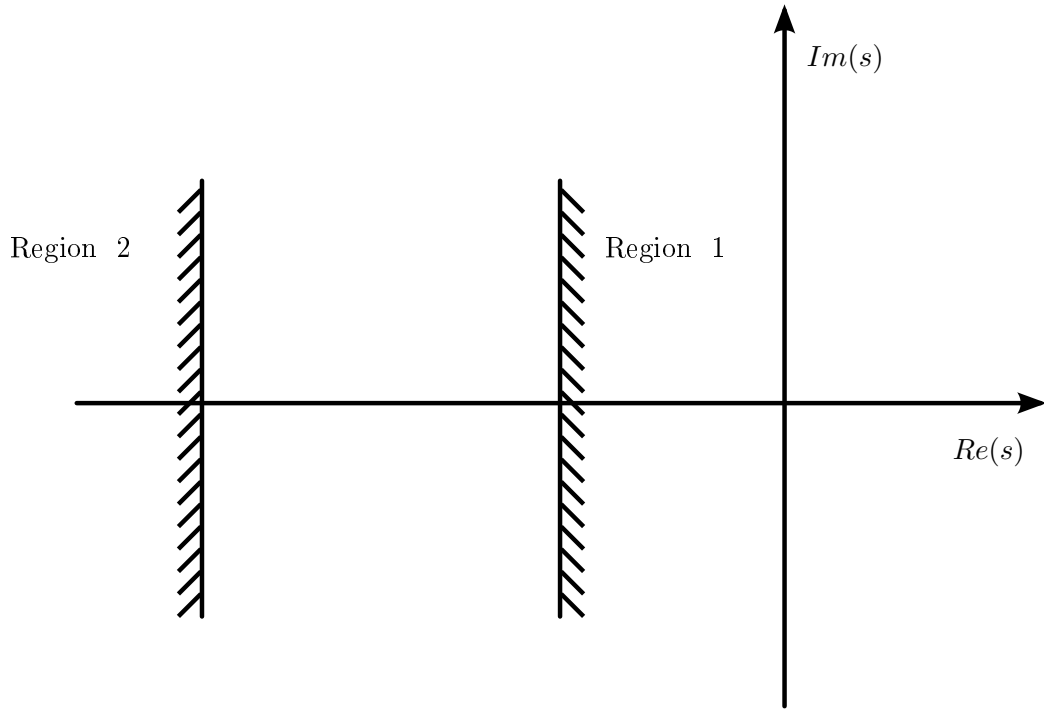
Figure 3.2: Regions of dominant and insignificant poles in the s-plane.

pair characterize the dynamics of the system. Low-frequency modes can be considered to achieve desired values of ζ and ω_n, and select the rest of the poles to increase the damping of high-frequency modes, while holding their frequency constant to minimize control efforts. It is important to consider that the zeros of the system should be far enough into the left half s-plane so as to avoid any appreciable effect on the second-order behavior of the system. The specifications of the relative stability and the speed of response are translated into a pair of the dominant closed-loop poles using the following relations. (Franklin et al., 2002),(Gopal, 2002)

$$\text{Rise time :} \qquad t_r = \frac{2.16\zeta + 0.60}{\omega_n}. \qquad (3.4)$$

$$\text{Peak time :} \qquad t_p = \frac{\pi}{\omega_n\sqrt{1 - \zeta^2}}. \qquad (3.5)$$

$$\text{Settling time (for 2\% criteria) :} \qquad t_s = \frac{4}{\zeta\omega_n}. \qquad (3.6)$$

Peak overshoot : $$M_p = e^{-\pi\zeta/\sqrt{1-\zeta^2}}.$$ (3.7)

The desired locations of the closed-loop poles are

$$s_{1,2} = -\zeta\omega_n \pm j\omega_n\sqrt{1 - \zeta^2}.$$ (3.8)

The design requirement is to force two of the closed-loop poles at the specified dominant positions and all other poles in the insignificant region. A simulation study can be performed to see whether the design is acceptable, if not, rearrange the design cycle to get a different distribution of the closed-loop poles. (Franklin et al., 2002),(Gopal, 2002)

3.2.2   Integral action

The state-feedback is a PD-type control. In order to reduce the steady state error, integral control is required. Consider a system, having a state-space model as shown in (2.7), (2.8) and $w = 0$. It is possible to feedback the integral of the error as well as the states of the plant, while augmenting the plant states with an extra (integral) state x_I (Franklin et al., 2002).

This extra integral state obeys the following differential equation

$$\dot{x_I} = \mathbf{C}\mathbf{x} - r,$$ (3.9)

where r is the reference input. Hence the integral state x_I is

$$x_I = \int^t e \; dt,$$ (3.10)

where e is the error. The augmented state equations for the system become

$$\begin{bmatrix} \dot{x_I} \\ \dot{\mathbf{x}} \end{bmatrix} = \begin{bmatrix} 0 & \mathbf{C} \\ \mathbf{0} & \mathbf{A} \end{bmatrix} \begin{bmatrix} x_I \\ \mathbf{x} \end{bmatrix} + \begin{bmatrix} 0 \\ \mathbf{B}_u \end{bmatrix} u - \begin{bmatrix} 1 \\ \mathbf{0} \end{bmatrix} r.$$ (3.11)

The feedback law is given as

$$u = -\begin{bmatrix} k_I & \mathbf{K} \end{bmatrix} \begin{bmatrix} x_I \\ \mathbf{x} \end{bmatrix}.$$ (3.12)

The block diagram of the system with the integral state x_I is represented as in Fig. 3.3.
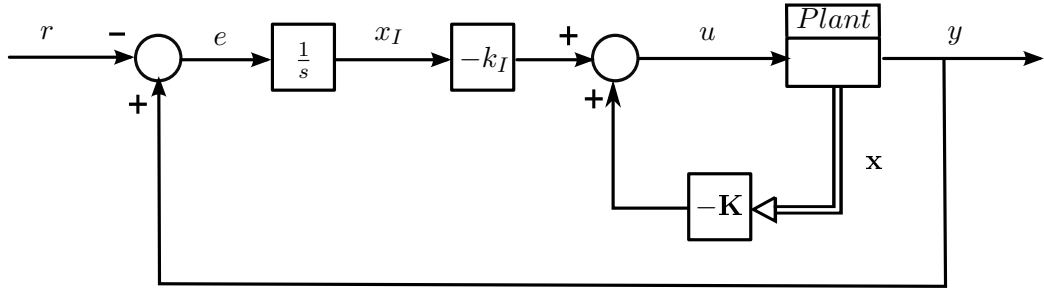
Figure 3.3: Integral control structure.

3.2.3   State-space controller

Considering a two-mass resonant system, a state-space controller is included in the system to make it a closed-loop system. The block diagram of the closed-loop system is shown in Fig. 3.4.

The gains can be calculated analytically from the closed-loop model. The state-space equations of the closed-loop system are given in (3.11) and (3.12) where k_I is the gain for the integral control and the gain matrix $\mathbf{K}$ is

$$\mathbf{K} = \begin{bmatrix} k_1 & k_2 & k_3 \end{bmatrix}, \qquad (3.13)$$

where k_1, k_2 and k_3 are the gains for ω_M, ε and ω_L, respectively.

The closed-loop system can be presented as

$$\begin{bmatrix} \dot{x}_I \\ \dot{\mathbf{x}} \end{bmatrix} = \underbrace{\begin{bmatrix} 0 & \mathbf{C} \\ -\mathbf{B}_u k_I & \mathbf{A} - \mathbf{B}_u \mathbf{K} \end{bmatrix}}_{\mathbf{A_{cl}}} \begin{bmatrix} x_I \\ \mathbf{x} \end{bmatrix} - \begin{bmatrix} 1 \\ \mathbf{0} \end{bmatrix} r. \qquad (3.14)$$

$$(3.15)$$

Eigenvalues (poles) of the closed-loop system can be calculated from the characteristic equation

$$B(s) = \det(s\mathbf{I} - \mathbf{A_{cl}}). \qquad (3.16)$$

The characteristics of the closed-loop system can be decided by the pole-placement design method. This closed-loop system with the integral control
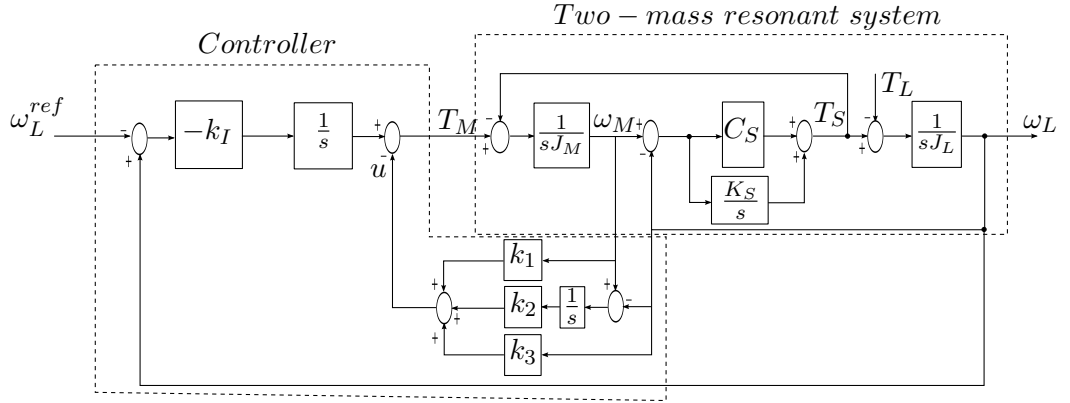
Figure 3.4: State-space controller of the two-mass resonant system with integral control.

becomes a fourth-order system. The characteristic equation of the system is

$$
B(s) = \overbrace{(s^2 + 2\zeta_1\omega_1 + \omega_1^2)}^{\textbf{Dominant}}\overbrace{(s^2 + 2\zeta_2\omega_2 + \omega_2^2)}^{\textbf{Resonant}}
$$
$$
= s^4 + 2(\zeta_1\omega_1 + \zeta_2\omega_2)s^3 + (\omega_1^2 + \omega_2^2 + 4\zeta_1\omega_1\zeta_2\omega_2)s^2
$$
$$
+ 2(\zeta_1\omega_1\omega_2^2 + \zeta_2\omega_2\omega_1^2)s + \omega_1^2\omega_2^2. \tag{3.17}
$$

ζ_1 and ω_1 decide the transient response of the system and ζ_2 and ω_2 are responsible for the resonance behavior of the system. Comparing (3.16) and (3.17), the following state-feedback gains can be found

$$
k_I = -\frac{J_L J_M \omega_1^2 \omega_2^2}{K_S} \tag{3.18}
$$

$$
k_1 = \frac{2J_L J_M(\zeta_1\omega_1 + \zeta_2\omega_2) - C_S(J_L + J_M)}{J_L} \tag{3.19}
$$

$$
k_2 = \frac{J_L J_M(\omega_1^2 + \omega_2^2 + 4\zeta_1\omega_1\zeta_2\omega_2) - C_S(k_1 + k_3) - K_S(J_L + J_M)}{J_L} \tag{3.20}
$$

$$
k_3 = \frac{2J_L J_M(\zeta_1\omega_1\omega_2^2 + \zeta_2\omega_2\omega_1^2) - K_S k_1 + C_S k_I}{K_S}. \tag{3.21}
$$

It is required to set the values of the tuning parameters ω_1, ω_2, ζ_1 and ζ_2 to calculate the gains for the state-space controller.
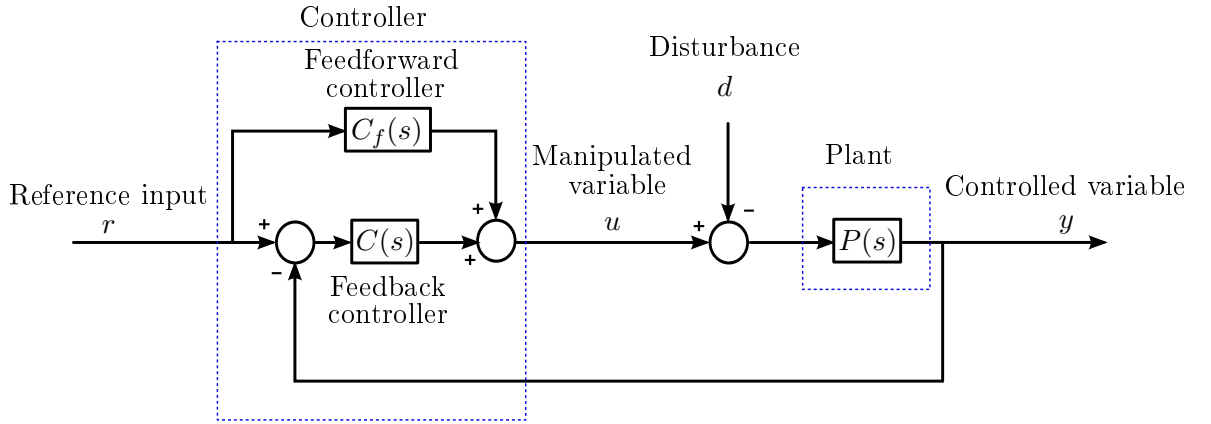
Figure 3.5: Two-degree-of-freedom-control system.

3.3   Two-degree-of-freedom controller design

The degree of freedom of a control system is defined as the number of the closed-loop transfer functions that can be adjusted independently. A general form of a 2DOF-control system is shown in Fig. 3.5. The control system consists of two controllers $C(s)$ and $C_f(s)$. In this control system, $C(s)$ is known as the feedback controller and $C_f(s)$ is called the feedforward controller. The $P(s)$ represents the plant to be controlled by the control system.

3.3.1   Feedback controller

Consider only the feedback controller and neglect the effect of the feedforward controller for the control system in Fig. 3.5. This arrangement makes this control system a one-degree-of-freedom (1DOF) control system. The closed-loop transfer function from the reference input r to the controlled output y and from the disturbance d to the controlled output y can be given as respectively

$$G_{yr1}(s) = \frac{P(s)C(s)}{1 + P(s)C(s)} \tag{3.22}$$

$$G_{yd1}(s) = -\frac{P(s)}{1 + P(s)C(s)}. \tag{3.23}$$

Here the subscript "1" indicates that these quantities are related to the 1DOF-control system. The two transfer functions, in (3.22) and (3.23), contain only one element that can be tuned, which is $C(s)$. Therefore, it is not

possible to change them independently. The relation of these two functions can be shown as

$$P(s) = G_{yr1}(s)P(s) - G_{yd1}(s). \qquad (3.24)$$

The equation shows that $G_{yr1}(s)$ can be determined uniquely for any given $P(s)$, provided $G_{yd1}(s)$ is chosen and vice versa. Hence, the reference input response becomes poor if the disturbance response is optimized and vice versa. Due to this fact, some researchers gave two separate tables for the optimal tuning of such controllers, where one is for the "disturbance optimal" parameters and the other for the "reference input optimal" parameters. (Chien et al., 1952)(R.Kuwata, 1987)

For the 1DOF-control system, it is not possible to optimize the reference input response and the disturbance response at the same time. This situation is shown in Fig. 3.6. The bold line indicates the Pareto optimal points for the 1DOF-control system. Only the hatched area in Fig. 3.6 is realizable by the 1DOF-control system. Here, points "A" and "B" are defined as:

- A is the disturbance optimal point.

- B is the reference input optimal point.

This limitation of the 1DOF-control structure compels to choose from these alternatives:

1. Choose one of the Pareto optimal points.

2. Use the disturbance optimal parameters and impose limitations on reference input variable change.

The second alternative is very useful for those systems where the reference input variable is not changed very often. This limitation can be avoided by using a 2DOF-control system instead. It provides good means to make both the reference input response and the disturbance response practically optimal at once within a linear framework. (Araki and Taguchi, 2003)

3.3.2   Feedforward controller

Consider the complete control system consisting of the feedback controller and the feedforward controller as shown in Fig. 3.5. This control system is a
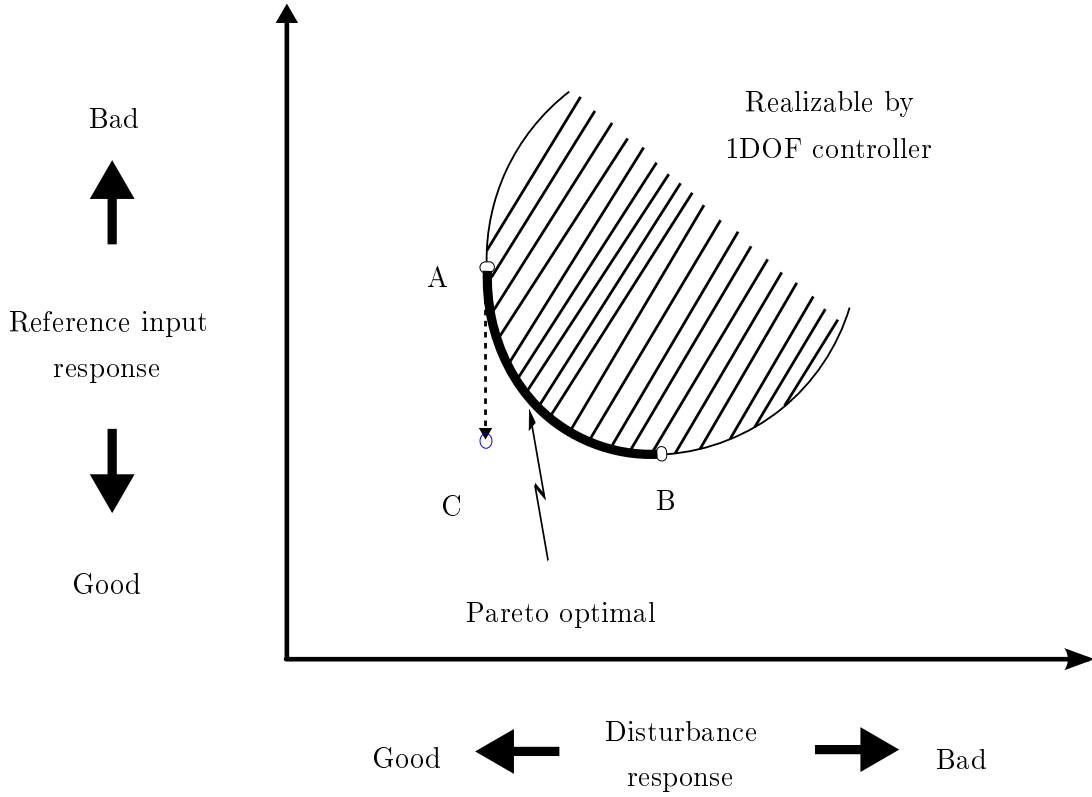
Figure 3.6: Conceptual illustration of the control structure's effect.

2DOF-control system. The closed-loop transfer functions from the reference input r to the output y and from the disturbance d to the output y are respectively

$$G_{yr2}(s) = \frac{P(s)[C(s) + C_f(s)]}{1 + P(s)C(s)Q(s)} \tag{3.25}$$

$$G_{yd2}(s) = G_{yd1}(s). \tag{3.26}$$

Here the subscript "2" indicates that these quantities are related to the 2DOF-control system. The steady state error to the unit step change of the reference input $\varepsilon_{r,step}$ and the steady state error to the unit step disturbance $\varepsilon_{d,step}$ becomes zero if the following conditions are fulfilled: (Araki and Taguchi, 2003)

$$\lim_{s \to 0} C(s) = \infty \tag{3.27}$$

$$\lim_{s \to 0} \frac{C_f(s)}{C(s)} = 0 \tag{3.28}$$

$$\lim_{s \to 0} P(s) \neq 0. \tag{3.29}$$

To satisfy these conditions, a simple case is that the $C(s)$ includes an integrator but the $C_f(s)$ does not contain any integrator. A number of topologies have been proposed considering the different industrial aspects for the 2DOF-control system: (Araki and Taguchi, 2003)

- Feedforward-type structure of the 2DOF-control system.

- Feedback-type structure of the 2DOF-control system.

- Set-point-filter-type structure of the 2DOF-control system.

- Filter and preceded-derivative type structure of the 2DOF-control system.

- Component separated type structure of the 2DOF-control system.

From all these categories, feedforward-type structure of the 2DOF-control system is of interest to us and it will be used in our design.

The feedforward-type structure of the 2DOF-control system is shown in Fig. 3.5. This structure is called feedforward-type due to the presence of a feedforward path from the reference input r to the manipulated variable u. The controller part is a two-input one-output system. The reference input r and the controlled output y are the input signals for the controller whereas the manipulated variable u is the output signal of the controller.

Comparing (3.22) and (3.23) with (3.25) and (3.26), it is seen that the closed-loop transfer functions for the 1DOF and the 2DOF-control systems are related to each other:

$$G_{yr2}(s) = G_{yr1}(s) + \frac{P(s)C_f(s)}{1 + P(s)C(s)}. \tag{3.30}$$

It can be concluded that

- The reference input response of the controllers differs by the amount of the second term in (3.30). This term can be changed by adjusting the $C_f(s)$.

- Both 1DOF and 2DOF-control systems have the same disturbance rejection response.

Hence, it is expected that from the 2DOF-control system, an improved reference input response can be obtained without deteriorating the disturbance response by appropriate tuning of the $C_f(s)$. For the 2DOF-control system, we can realize point "C" in Fig. 3.6. This clearly shows the advantage of the 2DOF-control system over the 1DOF-control system, providing more flexibility and improved results for the 2DOF-control system.(Araki and Taguchi, 2003)

3.4 2DOF controller for the two-mass resonant system

In this section, we will design a 2DOF controller for a two-mass resonant system described in Chapter 2. The structure of this 2DOF controller is of the feedforward type, including a feedback controller and a feedforward controller. We will use two different tuning techniques for the parameter selection of the 2DOF controller:

- Parameter tuning according to the rigid system model.

- Parameter tuning according to the flexible system model.

In the first tuning method, the two-mass resonant system is considered as a rigid system for the parameter tuning whereas in the second method, the flexible behavior of the two-mass resonant system is also taken into account for the parameter tuning.

The primary object in this control system design is to:

- Achieve fast tracking of the load speed with respect to the reference speed without overshoot.

- Reject the effect of the load torque.

In order to ensure the stability of the closed-loop system, there must be a bandwidth limitation of the feedback loop. It is also required to achieve the maximum possible bandwidth for the 2DOF speed controller. It is important to notice that in most industrial applications, where it is required to control the two-mass resonant system, measured information from the motor side is only available. The load information is not, usually, available. We will design the controller by considering the feedback signal from the motor instead of load, to control the load speed of the system.

3.4.1   Parameter tuning according to rigid system model

The feedforward type structure is used for this 2DOF-control system as shown in Fig. 3.5. In this tuning method we will model and analyze the plant by consideration of only the rigid part of the two-mass resonant system from (2.13). The first step in the design of a 2DOF controller is to design the feedback controller $C(s)$. The feedback controller $C(s)$ will be a PI controller which provides the stability and satisfactory performance with respect to the disturbances and the system uncertainties. The second step is to choose the feedforward controller $C_f(s)$ to shape the overall transfer function of the system as well as to obtain the desired command following specifications.

Feedback controller design

Consider Fig. 3.5 without taking into account the feedforward controller. The plant $P(s)$ is modeled considering only the rigid part and the feedback controller $C(s)$ is a PI controller. The reference input to the system is the reference load speed ω_L^{ref} and the controlled variable is the load speed ω_L.

$$C(s) = K_P + \frac{K_I}{s}. \tag{3.31}$$

$$P(s) = \frac{1}{s(J_M + J_L)}. \tag{3.32}$$

Considering (3.31) and (3.32), the closed-loop transfer function from ω_L^{ref} to ω_L is given as

$$\frac{\omega_L(s)}{\omega_L^{ref}(s)} = \frac{K_P}{J_M + J_L} \frac{s + \frac{K_I}{K_P}}{s^2 + (\frac{K_P}{J_M+J_L})s + \frac{K_I}{J_M+J_L}}. \tag{3.33}$$

Similarly, the closed-loop transfer function from T_L to ω_L is given as

$$\frac{\omega_L(s)}{T_L(s)} = \frac{-1}{J_M + J_L} \frac{s}{s^2 + (\frac{K_P}{J_M + J_L})s + \frac{K_I}{J_M + J_L}}. \tag{3.34}$$

The gains are analytically parameterized in terms of the inertia and the desired closed-loop bandwidth α_s. Hence, the values of K_P and K_I are given as

$$K_P = \alpha_s(J_M + J_L) \tag{3.35}$$

$$K_I = \left(\frac{\alpha_s}{2\zeta}\right)^2 (J_M + J_L). \tag{3.36}$$

where ζ is the damping coefficient of the system. Substituting the values of K_P and K_I in (3.33) and (3.34), a denominator polynomial for both transfer functions is obtained as

$$s^2 + \alpha_s s + \left(\frac{\alpha_s}{2\zeta}\right)^2. \tag{3.37}$$

Bandwidth selection

The bandwidth α_s should be less than the anti-resonance frequency of the two-mass resonant system. Considering the anti-resonance frequency from (2.18), the bandwidth of the system should be selected as

$$\alpha_s \leq \sqrt{\frac{K_S}{J_L}}. \tag{3.38}$$

The gains K_P and K_I of the 2DOF controller can be obtained from (3.35) and (3.36), by appropriate selection of bandwidth α_s and damping coefficient ζ of the system.

Feedforward controller design

When the main aim of the speed controlled system is to track the step-alike reference changes, only feedback controller (1DOF control structure) does not give sufficient results because of the overshoot. To reduce or eliminate

the overshoot appearing in the 1DOF control system, the structure can be modified by adding a feedforward controller $C_f(s)$ for the reference, to obtain the 2DOF-control system. The closed-loop transfer functions from the load speed reference ω_L^{ref} to the load speed ω_L becomes

$$P_c(s) = \frac{\omega_L(s)}{\omega_L^{ref}(s)} = \frac{C_f(s)P(s) + C(s)P(s)}{1 + C(s)P(s)}. \tag{3.39}$$

In principle, the closed-loop dynamics can be selected arbitrary by selecting a proper feedforward filter $C_f(s)$. In this case, tracking of the step-alike references is considered which leads to a selection of the first-order closed-loop dynamics. Furthermore, let us boost the dynamics of the closed-loop system m times. The dynamics of the closed-loop system is to be

$$P_c(s) = \frac{m\alpha_s}{s + m\alpha_s}. \tag{3.40}$$

The transfer function $C_f(s)$ can be solved from (3.39) and (3.40) by substituting the transfer functions of the process $P(s)$ and the PI controller $C(s)$:

$$C_f(s) = \frac{[(J_M + J_L)m\alpha_s - K_P]s - K_I}{s + m\alpha_s}. \tag{3.41}$$

If the PI controller parameters in (3.35) and (3.36) are substituted to (3.41), the transfer function $C_f(s)$ becomes

$$C_f(s) = \frac{(J_M + J_L)\alpha_s[(m-1)s - \frac{\alpha_s}{4\zeta^2}]}{s + m\alpha_s}. \tag{3.42}$$

Four special cases can be separated from (3.42):

- If the bandwidth of the 2DOF system is increased compared to the 1DOF design (i.e. $m > 1$), the feedforward filter $C_f(s)$ is a phase-lead filter.

- If the bandwidth of the 2DOF system is decreased compared to the 1DOF design (i.e. $m < 1$), the feedforward filter $C_f(s)$ is a phase-lag filter.

- If the bandwidth of the 2DOF system is the same as in the 1DOF design (i.e. $m = 1$), the feedforward filter is simply a low-pass filter.
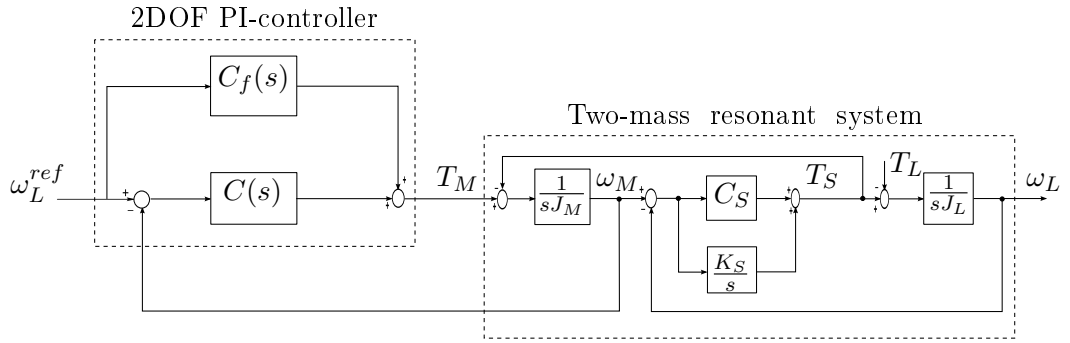
Figure 3.7: Detailed block diagram for 2DOF PI control of two-mass resonant system.

- If the bandwidth of the 2DOF system is half of the bandwidth in the 1DOF design and the feedback is critically damped (i.e. $m = 1/2$ and $\zeta = 1$), the feedforward filter is only a constant ($C_f(s) = -J\alpha_s/2$). This corresponds to the "active-damping" control design. (Harnefors et al., 2001)

It is also notable that if the bandwidth of the 2DOF controller is "boosted" ($m > 1$), the feedforward filter $C_f(s)$ will have an unstable zero so there will occur non-minimum phase behavior in the filter. In this thesis, we are considering the third special case and selecting the bandwidth of the 2DOF system as $m = 1$, leading to

$$C_f(s) = -\,\frac{(J_M + J_L)(\frac{\alpha_s}{2\zeta})^2}{s + \alpha_s}, \tag{3.43}$$

which is a first-order low-pass filter. The detailed block diagram of the closed-loop system, consisting of the 2DOF controller and the two-mass resonant system, is shown in Fig. 3.7.

By parameter selection of the feedforward controller from (3.43) and the parameter selection of the feedback controller from (3.35) and (3.36), the 2DOF speed controller can be tuned according to a rigid system model.

Dynamic references tracking

Especially in servo applications, the speed controlled system may not be driven with the step-alike references. Instead, for example the trapezoidal speed references are used, when the system is driven from one position to another. When the trapezoidal velocity reference is used, the speed of the

system is first accelerated to the constant value and then decelerated back to zero.

Let us study the tracking error of the 1DOF system and the 2DOF system if the system is accelerated with a constant acceleration α. This means that the speed reference is $\omega_L^{ref}(t) = \alpha t$, which is in the s-domain $\omega_L^{ref}(s) = \alpha/s^2$. The tracking error of the closed-loop system $P_c(s)$ can be expressed as

$$E(s) = \omega_L(s) - \omega_L^{ref}(s) = \omega_L^{ref}(s)[P_c(s) - 1]. \qquad (3.44)$$

Let us solve the steady-state tracking error for both the 1DOF and the 2DOF control structures. The closed-loop TF of the 1DOF control structure is

$$P_c(s) = \frac{\alpha_s s + (\frac{\alpha_s}{2\zeta})^2}{s^2 + \alpha_s s + (\frac{\alpha_s}{2\zeta})^2}. \qquad (3.45)$$

By substituting (3.45) and $\omega_L^{ref}(s) = \alpha/s^2$ to (3.44), the error becomes

$$E(s) = -\frac{\alpha}{s^2 + \alpha_s s + (\frac{\alpha_s}{2\zeta})^2}. \qquad (3.46)$$

The steady-state tracking error e_{ss} can be solved from (3.46) when applying the final value theorem

$$e_{ss} = \lim_{t\to\infty} e(t) = \lim_{s\to0} sE(s) = \lim_{s\to0}\left(-\frac{\alpha s}{s^2 + \alpha_s s + (\frac{\alpha_s}{2\zeta})^2}\right) = 0. \qquad (3.47)$$

By substituting (3.40) and $\omega_L^{ref}(s) = \alpha/s^2$ to (3.44), the error becomes

$$E(s) = -\frac{\alpha}{s(s + m\alpha_s)}. \qquad (3.48)$$

Futhermore, the steady-state tracking error e_{ss} is

$$e_{ss} = \lim_{s\to0}\left(-\frac{\alpha}{s + m\alpha_s}\right) = -\frac{\alpha}{m\alpha_s}. \qquad (3.49)$$

This brief analysis indicates that if the system is desired to follow the dynamic speed references, one should be careful when using the first-order closed-loop model. In this simple example, if the acceleration part is long enough, the tracking error of the 2DOF system will approach the value $\alpha/(m\alpha_s)$, when at the same time the tracking error of the 1DOF system will approach to zero.

3.4.2   Parameter tuning according to flexible system model

In the tuning method of a 2DOF PI controller presented by Zhang and Fu-rusho (2000), the two-mass resonant system is modeled as the flexible system. It is shown that three kinds of analytical pole placement techniques can be used. The relationship between the damping behavior and the inertia ratio is shown in Table 3.1.

Considering the inertia ratio from the two-mass system parameters presented in Table 2.1, we get

$$\text{Inertia ratio : R} = \frac{J_L}{J_M} = 8.18. \tag{3.50}$$

It is clear from Table 3.1, that only the pole assignment technique "identical damping coefficient" can be applied to this system as the inertia ratio is greater than 4. We will design the controller using an identical damping coefficient pole assignment technique as described by Zhang and Furusho (2000).

In order to compare both tuning methods, we will rearrange the block di-agram of the control system, presented by Zhang and Furusho (2000) in a feedforward type structure so that we can have a feedback controller $C(s)$ and feedforward controller $C_f(s)$. In the block digram of the system according to Zhang and Furusho (2000), the motor torque is given as

$$T_M(s) = \frac{K_I}{s}[\omega_L^{ref}(s) - \omega_M(s)] - K_P\omega_M(s). \tag{3.51}$$

Now, if we modify this system so as to use the common PI controller in the feedback loop and introduce the reference feed-forward filter, the motor torque is given as

$$T_M = \frac{K_I}{s}(\omega_L^{ref} - \omega_M) + K_P(\omega_L^{ref} - \omega_M) + F_r\omega_L^{ref}. \tag{3.52}$$

In order to get same expression for the motor torque, we have to select

$$C_f(s) = -K_P. \tag{3.53}$$

The modified block diagram for this control system, in terms of the feedfor-ward type structure, is shown in Fig. 3.7.

Controller gains

The closed-loop transfer function from the reference input ω_L^{ref} to the load speed ω_L is given as

$$\frac{\omega_L(s)}{\omega_L^{ref}(s)} = \frac{K_I \omega_A{}^2}{J_M s^2(s^2 + \omega_R^2) + (K_P s + K_I)(s^2 + \omega_A^2)}. \tag{3.54}$$

It is to be noted that this transfer function does not include the shaft damping coefficient C_S. Here ω_A is anti resonance frequency, ω_R is resonance frequency and R is the inertia ratio of the load to the motor and given as

$$\omega_R = \omega_A \sqrt{1 + R}. \tag{3.55}$$

The system in (3.54) can be arranged as

$$\frac{\omega_L(s)}{\omega_L^{ref}(s)} = \frac{\omega_1^2 \omega_2^2}{(s^2 + 2\zeta_1\omega_1 s + \omega_1^2)(s^2 + 2\zeta_2\omega_2 s + \omega_2^2)}, \tag{3.56}$$

where ω_1, ω_2 are the natural angular frequencies and ζ_1, ζ_2 are the damping coefficients. If we compare (3.54) and (3.56), we get following four equations

$$K_P = 2(\zeta_1\omega_1 + \zeta_2\omega_2)J_M \tag{3.57}$$

$$K_I = \frac{\omega_1^2 \omega_2^2}{\omega_A^2} J_M \tag{3.58}$$

$$\omega_A^2(\omega_1^2 + \omega_2^2 + 4\zeta_1\zeta_2\omega_1\omega_2) - \omega_1^2\omega_2^2 = \omega_A^4(R + 1) \tag{3.59}$$

$$\omega_1\zeta_1(\omega_2^2 - \omega_A^2) = \omega_2\zeta_2(\omega_A^2 - \omega_1^2). \tag{3.60}$$

Since we have only two adjustable feedback coefficients (K_p, K_I), it is not possible to assign the four poles arbitrarily. From (3.59) and (3.60), we get constraint relations among the pole locations. The pole locations are directly related to the inertia ratio R of the system as depicted by (3.59).

It is clear from (3.60) that

$$\min(\omega_1, \omega_2) \leq \omega_A \text{ and } \max(\omega_1, \omega_2) \geq \omega_A. \tag{3.61}$$
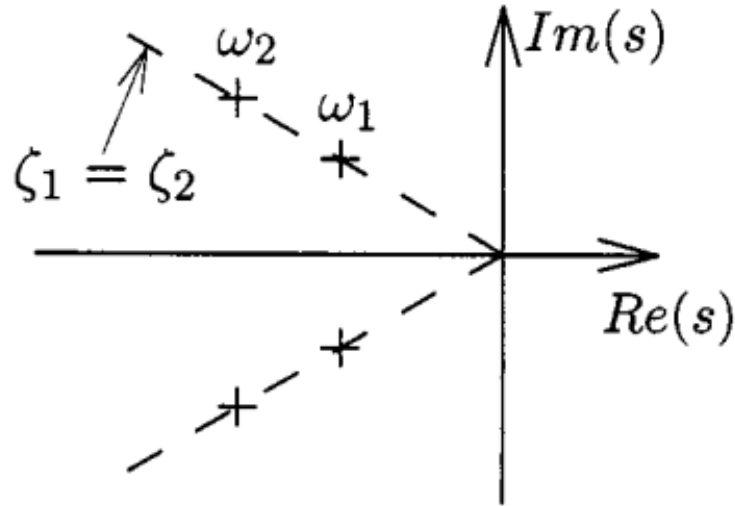
Figure 3.8: Pole assignment with identical damping coefficient (Zhang and Furusho, 2000).

Since the bandwidth of the system is determined by $\min(\omega_1, \omega_2)$, we cannot have the bandwidth more than the anti-resonance frequency ω_A of the system. (Zhang and Furusho, 2000)

Pole assignment of identical damping coefficient

The poles of the system (for dominant pole pair and resonant pole pair) are assigned to achieve identical damping coefficient as shown in Fig. 3.8. The dashed lines indicate the damping coefficient of both pole pairs. The frequencies of dominant pole pair and resonant pole pair move along these dashed lines where $\zeta_1 = \zeta_2$. It is shown by Zhang and Furusho (2000) that the overshoot of the system will gradually decrease with the increase of the identical damping coefficient. This can be observed clearly in Fig. 3.9. It is shown that the system overshoot is lower than 6.5% if the values of identical damping coefficients will be chosen as $\zeta_1 = \zeta_2 \geq 0.7$. The overshoot of the system will be within 2% if $\zeta_1 = \zeta_2 \geq 0.85$.

For the identical damping coefficients of the system, (3.59) and (3.60) can be reduced as
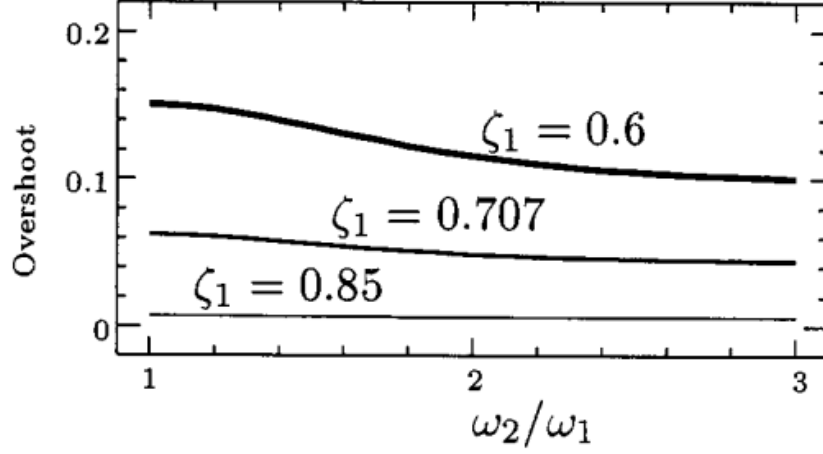
Figure 3.9: Overshoot for identical damping coefficient (Zhang and Furusho, 2000).

$$\left(\frac{\omega_A}{\omega_1} - \frac{\omega_1}{\omega_A}\right)^2 = R - 4\zeta_1^2 \tag{3.62}$$

$$\omega_2 = \frac{\omega_A^2}{\omega_1}. \tag{3.63}$$

We can derive ω_1 and ω_2 from (3.62) and (3.63) and given as

$$\omega_1 = \frac{\sqrt{R - 4\zeta_1^2 + 4} - \sqrt{R - 4\zeta_1^2}}{2}\omega_A \tag{3.64}$$

$$\omega_2 = \frac{\sqrt{R - 4\zeta_1^2 + 4} + \sqrt{R - 4\zeta_1^2}}{2}\omega_A. \tag{3.65}$$

Now ω_1 should be a nonnegative real number. Hence, we have to select the value of the damping coefficient as

$$\zeta_1 = \zeta_2 \leq \frac{\sqrt{R}}{2}. \tag{3.66}$$

If the value of the R is greater than or equal to 4, then the damping coefficient values can be assigned within 0 to 1 or $(1 - \frac{\sqrt{R}}{2})$. In this way, the four poles of

the system become the two pairs of complex conjugate roots, two double-real roots or four distinct real roots as per the selection of damping coefficient:

$$\text{Two pairs of complex conjugate} \quad : \quad \zeta_1 = \zeta_2 < 1 \qquad (3.67)$$

$$\text{Two double real roots} \quad : \quad \zeta_1 = \zeta_2 = 1 \qquad (3.68)$$

$$\text{Four distinct real roots} \quad : \quad \zeta_1 = \zeta_2 > 1 \qquad (3.69)$$

From these selections of parameters, the 2DOF controller can be tuned according to a flexible system model.

Chapter 4

Gain calculations and simulations

In this chapter, the simulation results for the three designed controllers, the state-space (SS) controller, the 2DOF controller with parameter tuning according to the rigid system model ($2DOF_{RSM}$) and the 2DOF controller with parameter tuning according to the flexible system model ($2DOF_{FSM}$) are presented. Finally, the responses of the three controllers are compared to each other for performance comparison.

4.1   Introduction to simulation models

In this section, the simulation models for the SS-control system and the 2DOF-control system are presented. The Matlab/Simulink software is used for the modeling and simulation of the speed control system. In the real systems, the encoders are also present in the complete drive system. This encoder, however, will add some noise in the system response. Hence, we have included an encoder model to incorporate the effect of the noise in the simulation results.

The input to the closed-loop system is the reference load speed ω_L^{ref} and the output is the load speed response of the system ω_L. The load reference speed input to the closed-loop system is stepped from 0 to 50 rad/sec at 0.1 second and the load torque is stepped from 0 to 10 Nm at 1.5 second.

In the simulation model, the main blocks of the model are the speed controller, the two-mass resonant system and the encoder model. The simulation model of the closed-loop system, including the state-space controller, the two-mass resonant system and the encoder model is shown in Fig. 4.1. The closed-loop system is modeled according to Fig. 3.4. The simulation model
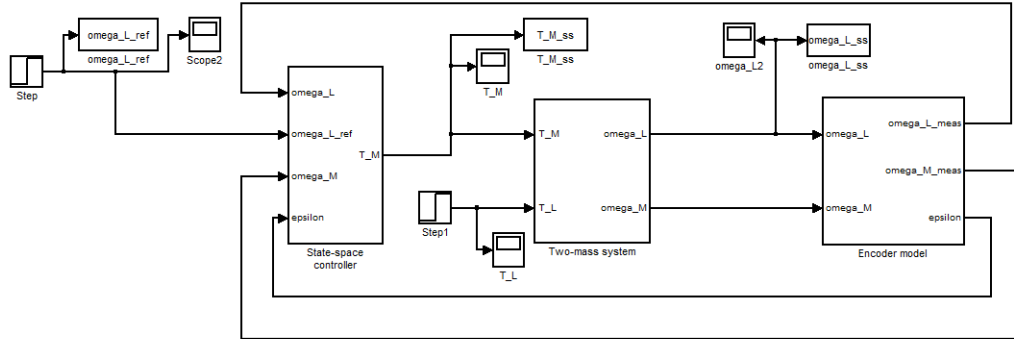
39

Figure 4.1: Simulation model of the state-space speed control system.

of the speed control system including the 2DOF controller, the two-mass resonant system and the encoder model is presented in Fig. 4.2. The speed control system is modeled according to Fig. 3.7.

4.2 Parameter gain selection

The designing rules for the selection of the gains for the controllers are described in Chapter 3. Considering those gain calculation rules, we will calculate the gains of the controllers by using the system parameters given in Table 2.1. First, we will find the aggressive design for all controllers to find the maximum bandwidth for each controller. Secondly, the response of the all controllers are examined to achieve the equivalent rise time. Finally, the controller parameters are adjusted to achieve the equivalent load torque rejection.

4.2.1 Aggressive design of the controllers

In order to calculate the gain values for the designed controllers to achieve the maximum bandwidth for 5% overshoot criteria, we are using the design rules as presented in Chapter 3 to calculate the gains for all controllers.

State-space controller's gains

It is clearly evident from (3.17), that the state-space speed control is a fourth-order system. we are considering the dominant pole pair method to select
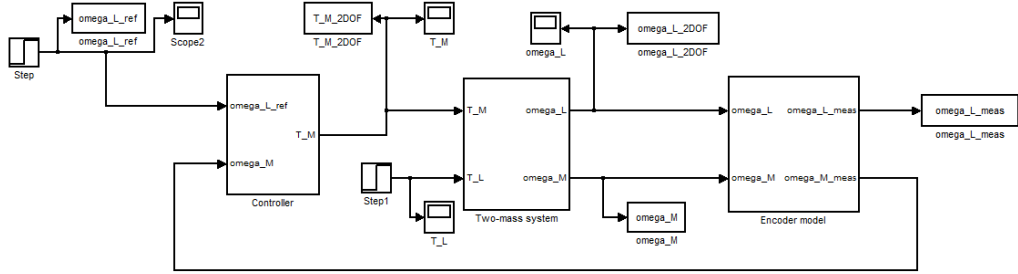
Figure 4.2: Simulation model of the 2DOF speed control system.

the frequencies and the damping ratios of the dominant and the resonant pole pairs. Considering that, the parameters ζ_1 and ω_1 are associated with the dominant pole pair and the parameters ζ_2 and ω_2 are associated with the resonant pole pair and represented as

$$\text{Dominant pole pair}\ :\qquad s^2 + 2\zeta_1\omega_1 + \omega_1{}^2 \qquad\qquad (4.1)$$

$$\text{Resonant pole pair}\ :\qquad s^2 + 2\zeta_2\omega_2 + \omega_2{}^2 \qquad\qquad (4.2)$$

The frequency of the resonant pole pair is selected equal to the undamped natural frequency of the system

$$\omega_2 = \omega_R = 87.5 \text{ rad/s.} \qquad\qquad (4.3)$$

Several simulations have been carried out, using different values of the damping ratios ζ_1 for the dominant pole pair, ζ_2 for the resonant pole pair and the maximum bandwidth of the system to analyze the behavior of the control system. The system response is well damped and has 5% overshoot for the values of the damping ratios and the frequencies as shown in Table 4.1.

Ideally, the overshoot can be reduced by increasing the value for the damping ratio of the resonant pole pair ζ_2 but in order to compare the response of the three designed controllers we have chosen the value of ζ_2 to get the overshoot in the system response. It is important to notice that, by selecting a small value of ζ_2 for the resonant pole pair, the gain values of the controller are not too high. It is in favor of good controller design to not select the high controller gains as the noise will be amplified by the high gains of the controller. For these gain selections, the maximum bandwidth ω_1 of the state-space controller of the two-mass resonant system is 73 rad/sec with 5%

Table 4.1: Parameters of dominant and resonant pole pairs.

Parameter	Dominant pole pair	Resonant pole pair
ζ_1	1	-
ζ_2	-	0.2
ω_1	73	-
ω_2	-	87.5

overshoot in the response. The gains for the state-space controller can be calculated by (3.18), (3.19), (3.20) and (3.21), considering the parameters of the dominant and the resonant pole pairs and the parameters of the system in Table 2.1.

2DOF controller's gains according to rigid system model

The gain calculation of the $2DOF_{RSM}$ controller depends on the bandwidth α_s and the damping coefficient ζ of the system whereas the bandwidth of the controller should be less than the anti-resonance frequency of the system. Several simulations have been carried out for the different values of α_s and ζ to analyze the behavior of the control system. The system response is well damped and within the required limits of 5% overshoot if the parameters are selected as

$$\alpha_s = 19 \text{ rad/sec} \tag{4.4}$$

$$\zeta = 1. \tag{4.5}$$

For these selections, the gains K_P, K_I of the controller can be calculated according to (3.35) and (3.36). The low-pass filter can be designed according to (3.43).

2DOF controller's gains according to flexible system model

The parameter selection of the $2DOF_{FSM}$ controller depends on the natural angular frequencies and the damping coefficients. The bandwidth of the system is determined by $\min(\omega_1, \omega_2)$. The bandwidth should be less than the anti-resonance frequency of the system. The natural frequencies ω_1 and ω_2

Table 4.2: Gain values of the designed controllers for aggressive design.

Gains	Speed controller type		
	$2DOF_{RSM}$	$2DOF_{FSM}$	SS
K_P	0.76	0.75	–
K_I	3.64	6.07	215.42
K_f	4.75	–	–
k_1	–	–	0.74
k_2	–	–	35.88
k_3	–	–	6.50
Bandwidth	19	11.76	73

are dependent on the damping coefficients of the system and these can be calculated by (3.64) and (3.65).

Using different damping coefficient values, several simulations for the control system have been performed to analyze the behavior of the system. The system response is well damped and within the required limits if we choose the values of damping coefficients as

$$\zeta_1 = \zeta_2 = 1. \tag{4.6}$$

By this selection of damping coefficients, the values of ω_1 and ω_2 are given as

$$\omega_1 = 11.76 \text{ rad/sec} \tag{4.7}$$

$$\omega_2 = 70.80 \text{ rad/sec}. \tag{4.8}$$

The gains K_P, K_I of the 2DOF controller, according to flexible system model tuning, can be calculated by (3.57), and (3.58). The bandwidth of the system is determined by $\min(\omega_1, \omega_2)$ so ω_1 is the maximum bandwidth of the system with 5% overshoot criteria. From the design rules and the parameter selections, the gain values of the three designed controllers are calculated and presented in Table 4.2.

Table 4.3: Gain values of the designed controllers for the equivalent rise time selection.

Gains	Speed controller type		
	$2DOF_{RSM}$	$2DOF_{FSM}$	SS
K_P	0.25	0.73	$-$
K_I	0.38	3.67	4.98
K_f	1.54	$-$	$-$
k_1	$-$	$-$	0.19
k_2	$-$	$-$	2.69
k_3	$-$	$-$	0.73
Bandwidth	6.15	11.76	11.1

4.2.2   Equivalent rise time for the controllers

In order to compare the rise time of all three controllers, the rise time is defined as "time taken for the output to rise from 0% to 90% of its final value when stimulated by a step input".

A number of simulations are done by changing the values of the bandwidth for the state-space controller and the $2DOF_{RSM}$ controller to obtain the equal rise time for all the controllers. The equivalent rise time is obtained if the bandwidth of the state-space controller is selected 11.1 rad/sec and the bandwidth of the $2DOF_{RSM}$ controller is selected 6.15 rad/sec. The remaining parameters of the controllers are selected similarly as in previous simulation. The equivalent rise time for all the controllers is 0.361 seconds. The gain values of the three designed controllers are calculated and presented in Table 4.3 for the equivalent rise time selection.

4.2.3   Equivalent load torque rejection for the controllers

The parameters of the $2DOF_{FSM}$ controller are adjusted similarly. The parameters of the state-space controller and the $2DOF_{RSM}$ controller will be selected to get the same load torque rejection according to the $2DOF_{FSM}$ controller.

Varying the different values of bandwidth of the controllers, several simulations are carried out to acquire the same load torque rejection. For the state-space controller, the damping coefficient value is also adjusted in addition to the bandwidth of the controller. All controllers have almost the same load

Table 4.4: Gain values of the designed controllers for the equivalent load torque rejection.

Gains	Speed controller type		
	$2DOF_{RSM}$	$2DOF_{FSM}$	SS
K_P	0.75	0.75	−
K_I	3.65	3.65	3.27
K_f	4.75	−	−
k_1	−	−	0.16
k_2	−	−	0.44
k_3	−	−	1.76
Bandwidth	19	11.76	9

torque rejection if the bandwidth of the $2DOF_{RSM}$ controller is chosen 19 rad/sec and the bandwidth of the state-space controller is selected 9 rad/sec with the damping coefficient value of the dominant pole pair chosen as 0.8. The remaining parameters of the controllers are selected similarly as in the previous simulation. The gain values of the three designed controllers are calculated and presented in Table 4.4 for the equivalent load torque rejection for the controllers.

4.3   Simulation results

The simulations are performed for the state-space controller, the $2DOF_{RSM}$ controller and the $2DOF_{FSM}$ controller using the gain values discussed in the previous subsections. In these simulations, the actual speed signals are shown.

4.3.1   Effect of encoder model

In the simulation models of the controllers, an incremental encoder is modeled and added in the closed-loop system. The purpose of the encoder is to add the noise effect in the system response. The comparison in the responses of the speed control system for the $2DOF_{FSM}$ controller is shown in Fig. 4.3 with noise and without noise due to the encoder model.

4.3.2 Aggressive design simulation

The gains of the all three controller are selected according to Table 4.2. The step response of the speed control system for each controller is shown in Fig. 4.4. This simulation is done for 5% overshoot criteria. In this case, our interest is to analyze the capability of the controllers to follow the reference signal efficiently. It is clearly visible from the simulation result that the state-space controller is fast as well as has the best load torque rejection among all the three controllers but there are some transients in the response of the system. The reason for these transients is that we are operating near the resonance area. The response of the $2DOF_{RSM}$ controller is fast as compared to the response of the $2DOF_{FSM}$ controller.

The load torque rejection is a little faster in the case of the 2DOF controller tuned according to the flexible system model as compared to the rigid system model tuning but it also has some overshoot after the recovery in the response. In case of rigid system model tuning, the load torque is slightly slower but it is well damped. In the motor torque T_M, maximum noise and maximum peak value of the torque is observed for the state-space controller. The reason for this noise is the fast response of the state-space controller. The $2DOF_{FSM}$ controller and the $2DOF_{RSM}$ controller have almost the same amount of noise but the latter has a high peak in the motor torque.

In the aggressive design simulation, the $2DOF_{RSM}$ controller han an edge of being fast in reference following as compared to the $2DOF_{FSM}$ controller. Both controllers have almost similar load torque rejection but the $2DOF_{RSM}$ controller has a high peak in the motor torque T_M.

4.3.3 Equivalent rise time simulation

The controller gains are selected as per Table 4.3. The step response of all three controllers is shown in Fig. 4.5. In this simulation, the rise time for all three control designs is fixed.

For equivalent rise time selection, no overshoot is observed in all three controllers. The noise in the motor torque is lowest for the $2DOF_{RSM}$ controller but it has very poor load torque rejection. The lowest noise is due to the small gain values of the controller. It also has the maximum peak in the motor torque T_M. On the other hand, the $2DOF_{FSM}$ controller has relatively high noise but the load torque rejection is good. The state-space controller has the highest noise of all three controller but it has the best load torque rejection.

In the equivalent rise time simulation, the $2DOF_{FSM}$ controller has significantly better results as compared to the $2DOF_{RSM}$ controller. There is a significant difference in the load torque rejection of both tuning techniques. In this case, one can easily conclude to prefer the $2DOF_{FSM}$ controller over the $2DOF_{RSM}$ controller.

4.3.4   Equivalent load torque rejection simulation

In order to get the equivalent load torque rejection for all the controllers, the gains are selected according to Table 4.4. The step response of all three controllers is shown in Fig. 4.6. It can clearly be observed from the simulation results that there is 4.4% overshoot in the response of the $2DOF_{RSM}$ controller and 1.2% overshoot in the response of the state-space controller for the same load torque rejection but there is no overshoot in the $2DOF_{RSM}$ controller response. The rise time of the $2DOF_{RSM}$ controller is the best of all the controllers but it has the maximum peak in the motor torque T_M. The noise is almost the same in response of all controllers.

In the equivalent load torque rejection (T_{lr}) simulation, the $2DOF_{FSM}$ controller shows better performance than the $2DOF_{RSM}$ controller. There is no overshoot in response as well as a low peak is observed in the motor torque for the $2DOF_{FSM}$ controller.
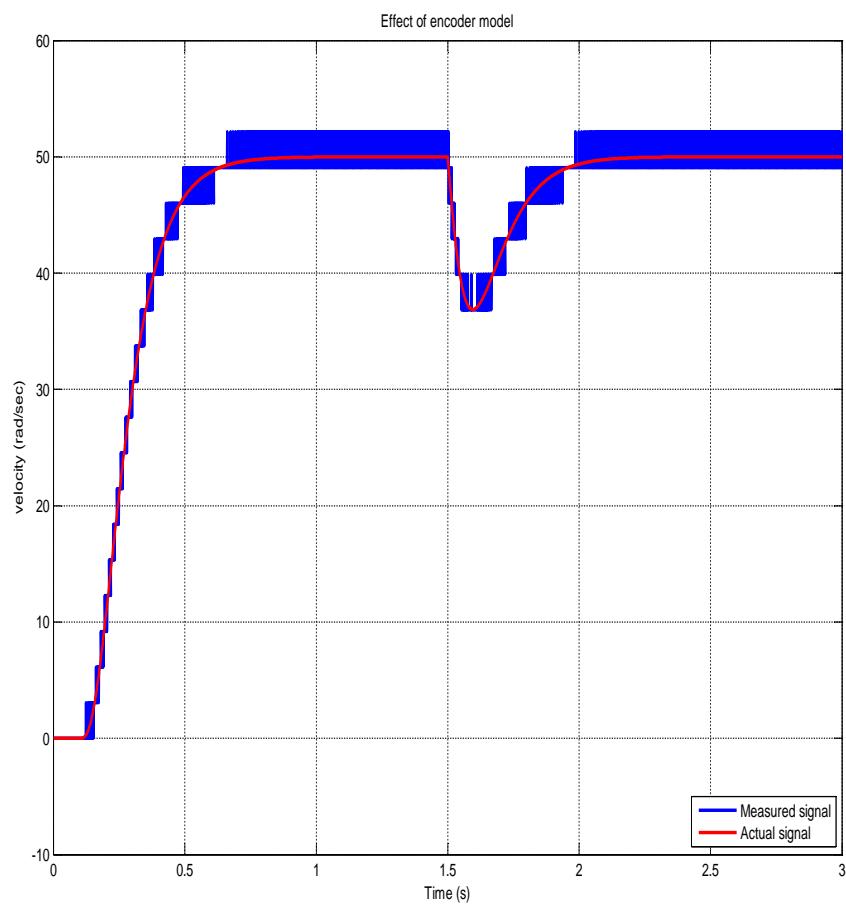
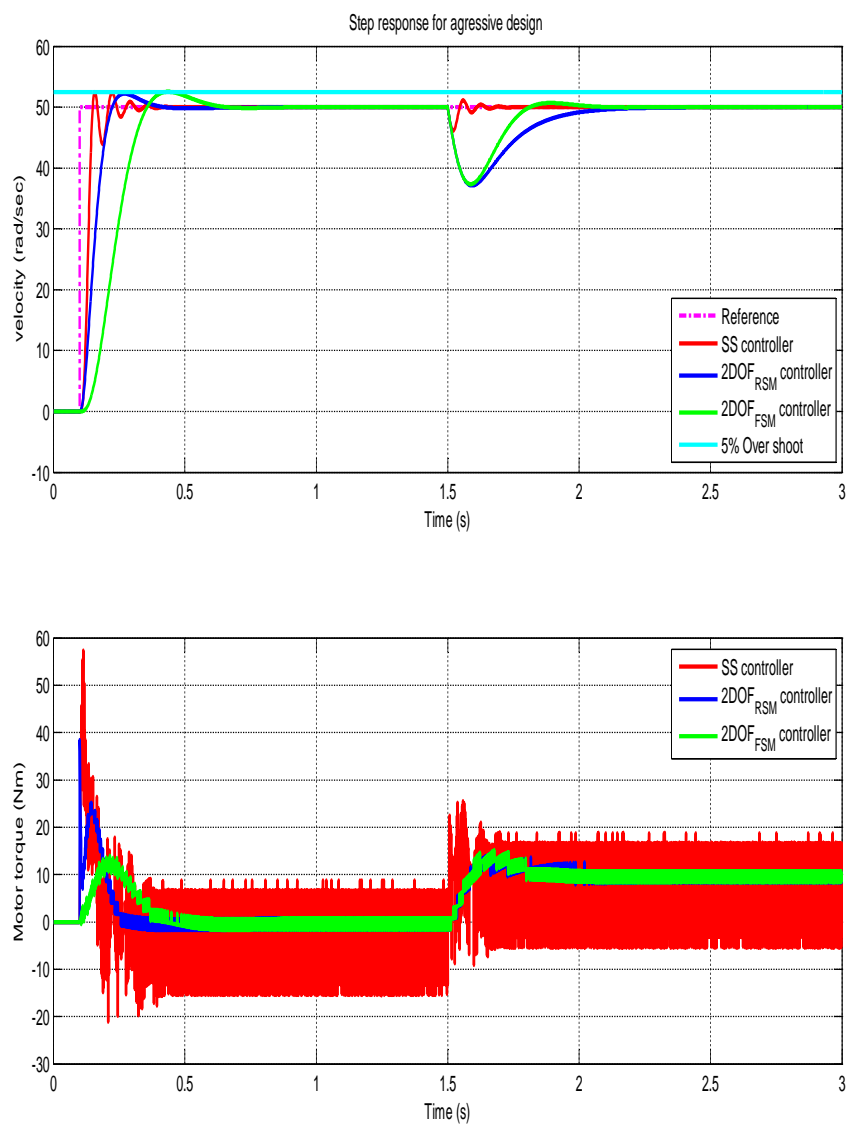Figure 4.3: The effect of the encoder model.

Figure 4.4: The step responses of the speed control system for the aggressive design.
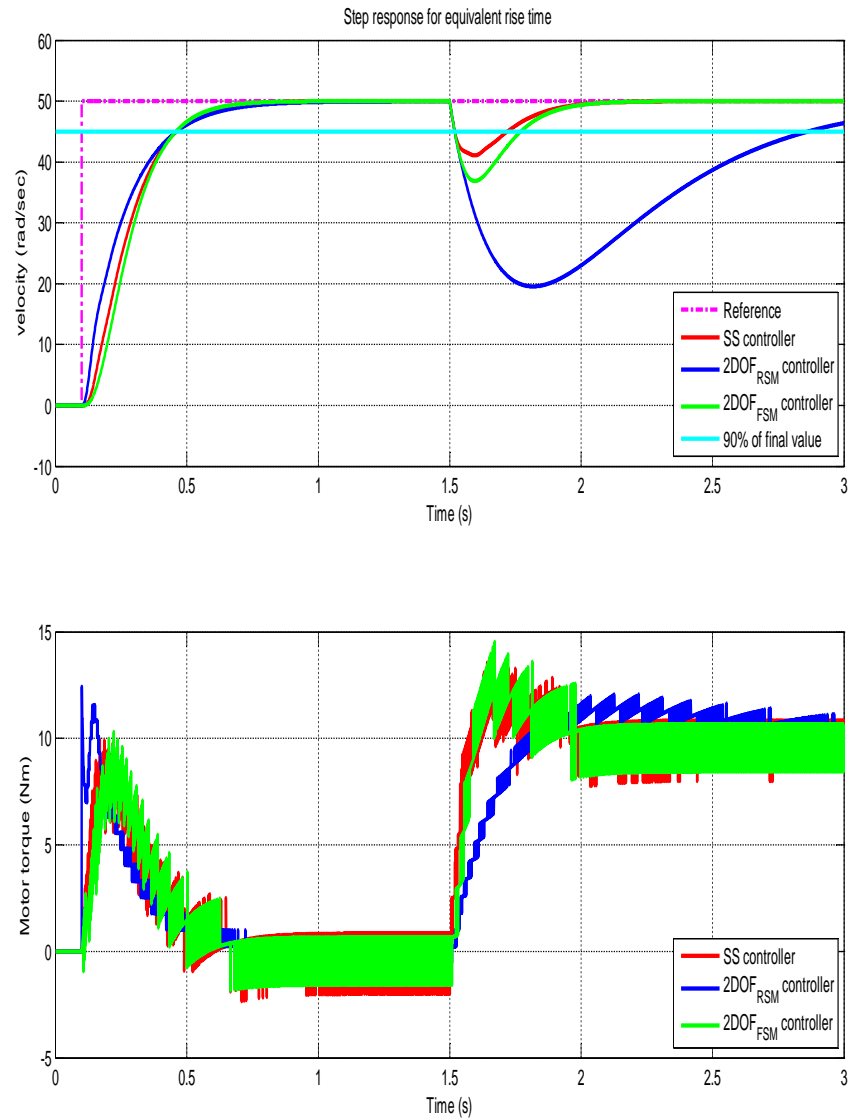
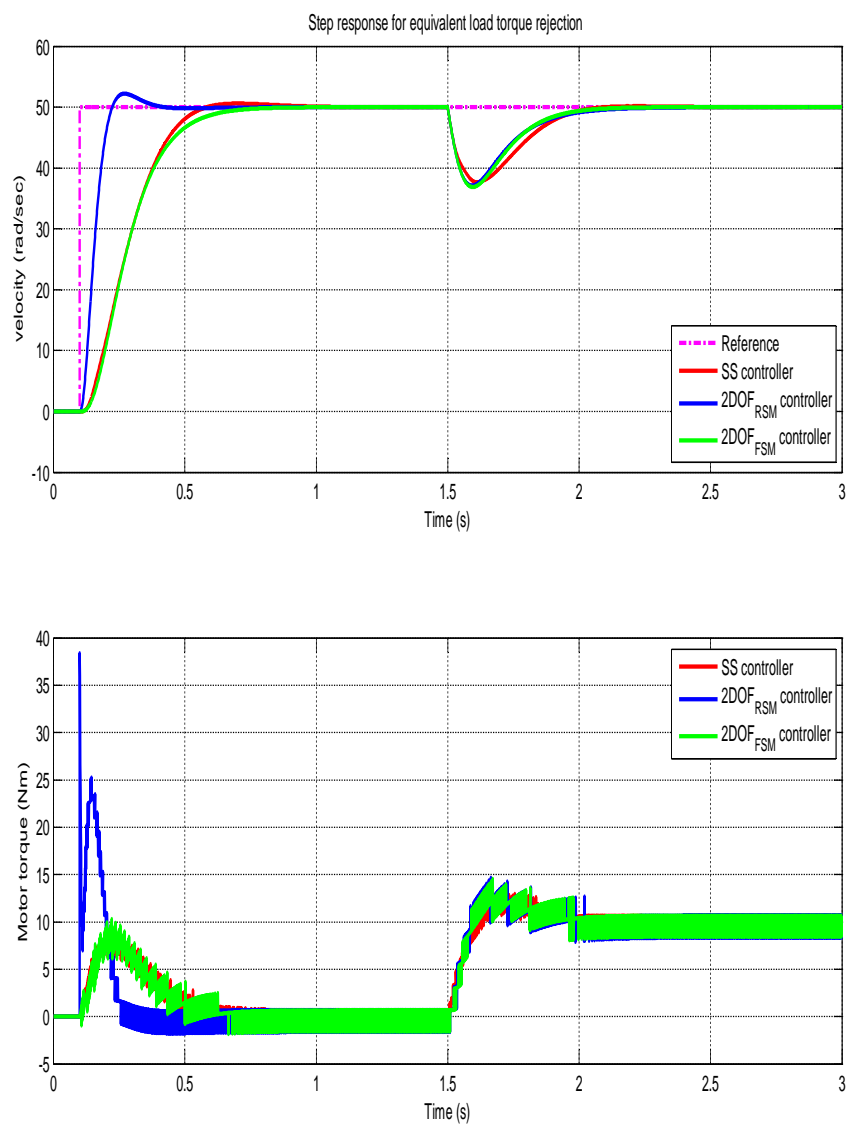Figure 4.5: The steps response of the speed control system for equivalent rise time.

Figure 4.6: The steps response of the speed control system for equivalent load torque rejection.

Table 4.5: Measured control performances.

Performance parameters	Controller	Agressive design	Equivalent rise time	Equivalent T_{lr}
T_r (sec)	SS	0.044	0.361	0.337
	$2DOF_{RSM}$	0.097	0.361	0.097
	$2DOF_{FSM}$	0.214	0.361	0.360
PO (%)	SS	5	−	1.2
	$2DOF_{RSM}$	5	−	4.4
	$2DOF_{FSM}$	5	−	−
T_{lr}	SS	best	best	Good
	$2DOF_{RSM}$	Good	Poor	Good
	$2DOF_{FSM}$	Good	Good	Good

4.4   Performance comparison

The simulation results are presented in Fig. 4.4, Fig. 4.5 and Fig. 4.6. The achieved control performances are characterized by the percentage overshoot (PO) in the response of the controllers, the rise time (T_r) and the load torque rejection (T_{lr}) of the controllers. The values of these performance parameters are summarized in Table 4.5 for each speed controller. The load torque rejection (T_{lr}) is characterized as best, good and poor considering best as the excellent and poor as the worst.

Chapter 5

Conclusions

The objective of this Master's thesis was to compare three speed controlling techniques for the two-mass resonant system: the state-space control, the 2DOF control tuned according to a rigid system model and the 2DOF control tuned according to a flexible system model. The control methods were designed and compared in terms of their dynamic behavior, reference following capability and load torque rejection. Furthermore, the effect of noise in the motor torque due to the encoder was also taken into account for each controlling technique.

The state-space controller is designed using the pole placement technique and analytical calculations are presented for the gains calculation. The feedforward type of 2DOF controller is first tuned considering the two-mass resonant system as a rigid system and then it is tuned according to a flexible system model. Analytical gain calculations for both tuning techniques are presented. Finally, three simulation studies are used to compare the performance of the designed speed controllers: the aggressive design simulation, the equivalent rise time simulation and the equivalent load torque rejection simulation.

It is observed that the best control performance can be achieved by the state-space controller due to its free pole placement property but it is required that all state variables should be available. Usually all state variables are not available and this condition will limit the performance of the state-space controller.

In the aggressive design simulation, the $2DOF_{RSM}$ controller has a faster reference following than the $2DOF_{FSM}$ controller for almost the same load torque rejection. It can be concluded that for the system where the fast rise time is required, the $2DOF_{RSM}$ controller will be preferred over the $2DOF_{FSM}$ controller but it is to be noted that there is a peak in the motor

torque for the $2DOF_{RSM}$ controller.

In the equivalent rise time simulation, the $2DOF_{FSM}$ controller had definitely better load torque rejection. The $2DOF_{RSM}$ controller has poor load torque rejection. Both tuning techniques have almost the same peak in motor torque but the flexible system model tuning has much more noise than the rigid system tuning. In this case the $2DOF_{FSM}$ controller shows better performances.

In the equivalent load torque rejection simulation, there is overshoot in the response of the $2DOF_{RSM}$ controller as well as a high peak in the motor torque but no overshoot is observed in the $2DOF_{FSM}$ controller's response. Hence, in this comparison, the $2DOF_{FSM}$ controller has a clear edge over the $2DOF_{RSM}$ controller.

The comparison of all three controllers with pros and cons is presented and the user has to decide, depending on the required control performance and the available control hardware, which of the control method is the most convenient one for their system. If future investigations in the area of the two-mass resonant system speed control are conducted, the study should concentrate on what the effect of state observers is on the state-space controller performance. For all controller tuning techniques, the robustness of the controllers to parameter variation can be analyzed. Further, it would be interesting to study the dynamical reference tracking capability of the controllers.

Bibliography

Araki, M. and Taguchi, H. (2003). Two degree of freedom PID controllers. *Proc. Inernational Journal of Control Automation and Systems*, 1(4):401–411.

Buchi, R. (2010). *State Space Control, LQR and Observer: Step by Step Introduction, with Matlab Examples*. Books on Demand GmbH, Hamberg, Germany, 1st edition.

Chien, K., Hrones, J. A., and Reswick, J. B. (1952). On the automatic control of generalized passive systems. *Trans. ASME*, 74:175–185.

Dhaouadi, R., Kubo, K., and Tobise, M. (1993). Two-degree-of-freedom robust speed controller for high-performance rolling mill drives. *IEEE Transaction on Industry Applications*, 29(5):919–923.

Dorf, R. C. and Bishop, R. H. (2001). *Modern Control Systems*. Prentice Hall, New Jersey, 9th edition.

Franklin, G. F., Powell, J. D., and Emami-Naeini, A. (2002). *Feedback Control of Dynamic Systems*. Prentice Hall, New Jersey, 4th edition.

Gopal, M. (2002). *Control Systems*. Tata McGraw-Hill, Delhi, India, 3rd edition.

Hara, K., Hashimoto, S., Funato, H., and Kamiyama, K. (1997). Robust comparison between state feedback-based speed control systems with and without state observers in resonant motor drives. In *International Conference on Power Electronics and Drives System, IEEE*, volume 1, pages 371–376.

Harnefors, L., Pietilainen, K., and Gertmar, L. (2001). Torque-maximizing field-weakening control: design, analysis, and parameter selection. *Industrial Electronics, IEEE Transactions on*, 48(1):161–168.

Kim, Y.-S., Kim, S.-B., Kim, J.-S., Yoo, C.-H., and Kim, H.-J. (1996). Two-degree-of-freedom speed control of induction motor having two-mass resonant system. In *Industrial Electronics, Control, and Instrumentation, 1996., Proceedings of the 1996 IEEE IECON 22nd International Conference on*, volume 2, pages 1210 –1215.

Lee, S.-H., Hur, J.-S., Cho, H.-C., and Park, J.-H. (2006). A PID-type robust controller design for industrial robots with flexible joints. In *SICE-ICASE, 2006. International Joint Conferencen*, pages 5905 –5910.

Leonhard, W. (1996). *Control of Electrical Drives.* Springer-Verlag, Berlin,Germany, 2nd edition.

Orlowska-Kowalska, T., Dybkowski, M., and Szabat, K. (2010). Adaptive sliding-mode neuro-fuzzy control of the two-mass industion motor drive withour mechanical sensor. *IEEE Transactions on Industrial Electronics*, 57(2):553–563.

R.Kuwata (1987). An improved ultimate sensitivity method and PID: characteristics of I-PD control. *Trans. SICE*, 23:232–239.

Shahgholian, G., Faiz, J., and Shafaghi, P. (2009a). Analysis and simulation of speed control for two-mass resonant system. In *Proc. ICCEE'09*, pages 666 – 670, Dubai, UAE.

Shahgholian, G., Shafaghi, P., Zinali, M., and Moalem, S. (2009b). State space analysis and control of two-mass resonant system. In *Proc. ICCEE'09*, pages 97 – 101, Dubai, UAE.

Szabat, K. and Kowalska, T. O. (2007). Vibration suppression in a two-mass drive system using PI speed controller and additional feedbacks-comparative study. *IEEE Transactions on Industrial Electronics*, 54(2):1193–1206.

Thomsen, S., Hoffmann, N., and Fuchs, F. (2010). Comparative study of conventional PI-control, PI based state space control and model based predictive control for drive systems with elastic coupling. In *Energy Conversion Congress and Exposition (ECCE), IEEE*, pages 2827 – 2835, Atlanta, GA.

Wang, Q.-G., Zhang, Z., Astrom, K. J., and Chek, L. S. (2009). Guaranteed dominant pole placement with PID controllers. *Journal of Process Control*, 19(2):349–352.

Zhang, G. and Furusho, J. (2000). Speed control of two-inertia system by PI/PID control. *IEEE Trans. Ind. Electron.*, 47(3):603–609.